PREPARATION AND OPERATIONS OF THE MISSION PERFORMANCE CENTRE (MPC) FOR THE COPERNICUS SENTINEL-3 MISSION

S3 Wind and Waves Cyclic Performance Report

S3-A	S3-B
Cycle No. 045	Cycle No. 026
Start date: 17/05/2019	Start date: 27/05/2019
End date: 13/06/2019	End date: 23/06/2019

SENTINEL 3

Mission Performance Centre

Ref.: S3MPC.ECM.PR.07-045-026

Issue: 1.0

Date: 28/06/2019

Contract: 4000111836/14/I-LG

Customer:	ESA	**Document Ref.:**	S3MPC.ECM.PR.07-045-026
Contract No.:	4000111836/14/I-LG	**Date:**	28/06/2019
		Issue:	1.0

Project:	PREPARATION AND OPERATIONS OF THE MISSION PERFORMANCE CENTRE (MPC) FOR THE COPERNICUS SENTINEL-3 MISSION		
Title:	S3 Wind and Waves Cyclic Performance Report		
Author(s):	Saleh Abdalla		
Approved by:	G. Quartly, STM ESL Coordinator	**Authorized by**	Sylvie Labroue, STM Technical Performance Manager
Distribution:	ESA, EUMETSAT, S3MPC consortium		
Accepted by ESA	P. Féménias, MPC TO		
Filename	S3MPC.ECM.PR.07-045-026 - i1r0 - WindsWaves Cyclic Report 045-026.docx		

Disclaimer

The work performed in the frame of this contract is carried out with funding by the European Union. The views expressed herein can in no way be taken to reflect the official opinion of either the European Union or the European Space Agency.

Changes Log

Version	Date	Changes
1.0	28/06/2019	First Version

List of Changes

Version	Section	Answers to RID	Changes

Table of content

1 SUMMARY 1

2 EVENTS 2

3 DATA PROCESSING 5

4 RADAR BACKSCATTER AND SURFACE WIND SPEED 6

4.1 BACKSCATTER 6

4.2 SAR MODE SURFACE WIND SPEED 7

4.3 PLRM SURFACE WIND SPEED 18

5 SIGNIFICANT WAVE HEIGHT 24

6 CONCLUSIONS 36

7 REFERENCES 38

8 APPENDIX A: VERIFICATION APPROACH 39

8.1 INTRODUCTION 39

8.2 QUALITY CONTROL PROCEDURE 40

8.3 BASIC QUALITY CONTROL 40

8.4 CONSISTENCY QUALITY CONTROL 43

8.5 OUTPUT FILES 44

8.6 ALTIMETER MODEL COLLOCATION 45

8.7 ALTIMETER BUOY COLLOCATION 45

9 APPENDIX B: RELATED REPORTS 47

List of Figures

Figure 1: Sentinel-3A SRAL ocean Ku-band backscatter histogram (PDF) over the whole globe and for the period from 27/05/2019 to 23/06/2019 which corresponds to Cycle 026-B of Sentinel-3B and a 10-day shifted-ahead Cycle 045-A (045-A+10) of Sentinel-3A. For comparison, the same plot from the previous Sentinel-3B cycle is also shown.---------- 6

Figure 2: Time series of global mean (top) and standard deviation (bottom) of backscatter coefficient of SRAL Ku-band from both Sentinel-3A and Sentinel-3B after quality control. Mean and SD are computed over a moving time window of 7 days and are shown as thin lines. The 92-day running means are shown as thick lines.---------- 7

Figure 3: Sentinel-3 SRAL SAR surface wind speed PDF's over the whole global ocean and for the period from 27/05/2019 to 23/06/2019 which corresponds to Cycle 026-B of Sentinel-3B and a 10-day shifted-ahead Cycle 045-A (045-A+10) of Sentinel-3A. The corresponding ECMWF (collocated with Sentinel-3) PDF's are also shown for comparison. The corresponding PDF's (SRAL and model) from the previous Sentinel-3B cycle are also shown as dashed lines. ---------- 8

Figure 4: Global comparison between Sentinel-3 SRAL and ECMWF model analysis surface wind speed values over the period from 27/05/2019 to 23/06/2019 which corresponds to a 10-day shifted-ahead Cycle 045-A (045-A+10) of Sentinel-3A (a) and Sentinel-3B Cycle 026-B (b). The number of collocations in each 0.5 m/s x 0.5 m/s 2D bin is color-coded as in the legend. The crosses are the means of the bins for given x-axis values (model) while the circles are the means for given y-axis values (Sentinel-3).---------- 9

Figure 5: Same as Figure 4 but for Northern Hemisphere (north of 20° N), Tropics (20° S - 20° N) and Southern Hemisphere (south of 20° S), respectively. Sentinel-3A plots on the left-hand side while S-3B plots on the right.----------11

Figure 6: Time series of global mean (top) and standard deviation (bottom) of wind speed from SRAL Ku-band after quality control from both Sentinel-3A and Sentinel-3B. The collocated model wind speed mean and SD are also shown. Mean and SD are computed over a moving time window of 7 days (shown as thin lines). The 92-day running means are shown as thick lines.----------12

Figure 7: Time series of weekly wind speed bias defined as altimeter - model (top) and standard deviation of the difference (bottom) between Sentinel-3A SRAL Ku-band and ECMWF model analysis. -13

Figure 8: Same as Figure 7 but for Sentinel-3B. ----------13

Figure 9: Geographical distribution of mean Sentinel-3A wind speed (a) as well as the bias (b); the SDD (c) and the SI (d) between Sentinel-3A and ECMWF model AN during the period from 27/05/2019 to 23/06/2019 which corresponds to a 10-day shifted-ahead Cycle 045-A (045-A+10) of Sentinel-3A. Bias is defined as altimeter – model. ----------14

Figure 10: Same as Figure 9 but for Sentinel-3B Cycle 026-B from 27/05/2019 to 23/06/2019. ----------16

Figure 11: Same as Figure 4 but the comparison is done against in-situ observations (mainly in the NH).19

Figure 12: Global comparison between Sentinel-3 PLRM and ECMWF model analysis wind speed values over the period from 27/05/2019 to 23/06/2019 which corresponds to a 10-day shifted-ahead Cycle

045-A (045-A+10) of Sentinel-3A (a) and Sentinel-3B Cycle 026-B (b). Refer to Figure 4 for the meaning of the crosses and the circles as well as the colour coding. ----------20

Figure 13: Same as Figure 12 but for (a) Northern Hemisphere (north of 20° N), (b) Tropics (20° S - 20° N) and (c) Southern Hemisphere (south of 20° S), respectively. Sentinel-3A plots on left-hand side while 3B plots on right.----------21

Figure 14: Time series of weekly PLRM wind speed bias defined as altimeter - model (top) and standard deviation of the difference (bottom) between Sentinel-3A SRAL PLRM and ECMWF model analysis.-----22

Figure 15: Same as Figure 14 but for Sentinel-3B.----------23

Figure 16: Sentinel-3 SRAL SWH PDF's over the whole global ocean and for the period from 27/05/2019 to 23/06/2019 which corresponds to Cycle 026-B of Sentinel-3B and a 10-day shifted-ahead Cycle 045-A (045-A+10) of Sentinel-3A. The corresponding ECMWF (collocated with Sentinel-3) PDF's are also shown for comparison. The corresponding PDF's from the previous Sentinel-3B cycle are shown as dashed lines.24

Figure 17: Global comparison between Sentinel-3 and ECMWF model first-guess significant wave height values over the period from 27/05/2019 to 23/06/2019 which corresponds to a 10-day shifted-ahead Cycle 045-A (045-A+10) of Sentinel-3A (a) and Sentinel-3B Cycle 026-B (b). The number of colocations in each 0.25 m x 0.25 m 2D bin is coded as in the legend. Refer to Figure 4 for the meaning of the crosses and the circles. ----------26

Figure 18: Same as Figure 17 but for Northern Hemisphere (latitudes to the north of 20° N), Tropics (latitudes between 20° S and 20° N) and Southern Hemisphere (latitudes to the south of 20° S), respectively.----------27

Figure 19: Time series of global mean (top) and standard deviation (bottom) of significant wave height from SRAL Ku-band after quality control. The collocated ECMWF model SWH mean and SD are also shown. The mean and SD are computed over a moving time window of 7 days and are shown as thin lines. The 92-day running means are shown as thick lines. ----------28

Figure 20: Time series of weekly global significant wave height bias defined as altimeter - model (top) and standard deviation of the difference (bottom) between SRAL and ECMWF model first-guess.--------29

Figure 21: Same as Figure 20 but for Sentinel-3B.----------29

Figure 22: Geographical distribution of mean Sentinel-3A SWH (a) as well as the bias (b); the SDD (c) and the SI (d) between Sentinel-3 and ECMWF model FG during the period from 27/05/2019 to 23/06/2019 which corresponds to a 10-day shifted-ahead Cycle 045-A (045-A+10) of Sentinel-3A. Bias is defined as altimeter – model.----------31

Figure 23: Same as Figure 22 but for Sentinel-3B Cycle 026-B from 27/05/2019 to 23/06/2019.----------33

Figure 24: Same as Figure 17 but the comparison is done against in-situ observations (mainly in the NH).35

List of Tables

Table A.1: QC Parameters for Altimeter Data from Various Satellites----------39

Table A.2: The Standard Quality Flags used in the Quality Control Procedure. A flags is raised (i.e. set to 1) to indicate an issue. An observation record passes QC if all general flags except flag 6 are not raised (i.e. set to zero). SWH and wind speed have their own specific flags.----------41

1 Summary

This is a cyclic report on the quality of wind and wave observations and their timely availability from the radar altimeter SRAL on-board:

- Sentinel-3A for Cycle No. 045 covering the period from 17/05/2019 to 13/06/2019. For better comparison with Sentinel-3B some of the plots show results from a cycle shifted by 10 days (referred to as 045+10) to coincide with Sentinel-3B Cycle No. 026, i.e. from 27/05/2019 to 23/06/2019); and
- Sentinel-3B for Cycle No. 026 (period from 27/05/2019 to 23/06/2019).

The product under consideration is the Level 2 Marine Ocean and Sea Ice Areas (SRAL-L2MA) also referred to as S3A_SR_2_WAT that is nominally distributed in near real time (NRT). This work covers the Cal/Val Task SRAL-L2MA-CV-230 (Wind, wave product validation vs models).

Radar backscatter (sigma0), surface wind speed (WS) and significant wave height (SWH) from product S3A_SR_2_WAT are monitored and validated using the procedure used successfully for the validation of the equivalent products from earlier altimeters. The procedure is described in Appendix A. The procedure composed of a set of self-consistency checks and comparisons against other sources of data. Model equivalent products from the ECMWF Integrated Forecasting System (IFS) and in-situ measurements available in NRT through the Global Telecommunication System (GTS) are used for the validation.

2 Events

The major changes and events that may had impact on the results of the validation of Sentinel-3 wind and wave products presented in this report are listed below (items in **bold are satellite related**):

- **16 February 2016**: **Launch of Sentinel-3A**
- 08 Mar 2016: Model change to CY41R2. The main change is the implementation of the new 9-km cubic octahedral grid ($T_{CO}1279$) for the high-resolution configuration of IFS.
- **09 April 2016**: **Switch SRAL to LRM Mode**
- **12 April 2016**: **Switch SRAL back to SAR Mode**
- **14 October 2016**: **Implementation of SRAL processing chain IPF-SM-2 version 06.03**
- **17 November 2016**: **Implementation of SRAL processing baseline (PB) 2.09 which includes processing chain IPF versions 06.07 and 06.05 for Level-1 and Level-2, respectively.**
- 22 November 2016: ECMWF model changed to CY43R1. This change has almost no impact on the products assessed here.
- **29 November 2016**: **ADF SR_2_CON_AX (SM-2) Ver. 006: SAR Sigma0 increased by 0.35 dB and PLRM Sigma0 increased by 0.1 dB.**
- **05 December 2016**: **Implementation of further changes to the processing chain "SRAL/MWR L2 IPF (SM-2) Ver. 06.05"**
- **12 January 2017** **Implementation of Level-1 IPF version 06.09.**
- **28 February 2017** **Implementation of PB 2.10 which includes: Level-1 IPF version 06.10, MWR IPF version 06.03 and Level-2 IPF version 06.06. Updated calibrations were introduced.**

- **12 April 2017** **Implementation of PB 2.12 which includes Level-1 IPF version 06.11 and Level-2 IPF version 06.07. The change targeted the generation of Level-1b-S products with no impact on Level-2 products.**
- 11 July 2017 ECMWF model changed to CY43R3. This change has almost no impact on the products assessed here. However, it impacted the corrections computed from the model fields like dry and wet tropospheric corrections.
- **13 December 2017** **Implementation of PB 2.24 which includes: Level-1 IPF version 06.12, MWR IPF version 06.04 and Level-2 IPF version 06.106. Relevant changes include: aligning ocean Ku-band sigma0 (all modes: LRM, PLRM & SAR) Envisat mean value (10.8 dB without the atmospheric attenuation); correcting sigma0 for atmospheric attenuation; reducing SAR Ku-band SWH overestimation (SAMOSA 2.5 retracker).**
- **14 February 2018** **Implementation of PB 2.27 which includes: updates of on-ground calibration strategy to improve data quality and reduce noise; and direct computation of significant wave height from SAMOSA retracker outputs in addition to few bug-fixes.**
- **04 April 2018** **Implementation of PB 2.33.**
- **25 April 2018**: **Launch of Sentinel-3B**
- **10 May 2018**: **Switch Sentinel-3B SRAL to LRM Mode**
- 06 June 2018: ECMWF model changed to CY45R1.
- **07 June 2018**: **Switch Sentinel-3B SRAL back to SAR Mode**
- **16 October 2018**: **End of Sentinel-3B tandem phase with Sentenel-3A**
- **23 November 2018** **End of Sentinel-3B second drift phase when it reached its definitive orbit**
- **06 December 2018** **Implementation of Sentinel-3B PB 1.13**
- **14 February 2019** **Implementation of Sentinel-3A PB-2.45 and Sentinel-3B PB 1.17. This PB update is expected to have an impact on significant wave height.**

- 11 June 2019: ECMWF model changed to CY46R1 which includes significant improvements to the wave model mainly related swell development.

All ECMWF Integrated Forecast System (IFS) model changes are summarised at:
http://www.ecmwf.int/en/forecasts/documentation-and-support/changes-ecmwf-model

3 Data Processing

The validation is based on the NRT operational Sentinel-3 (both 3A and 3B) Surface Topography Mission Level 2 (S3-A STM L2) wind and wave marine products (S3A_SR_2_WAT) product. For the time being, the product distributed by EUMETSAT in netCDF through their Online Data Access (ODA) system is used after converting into ASCII format but this will be replaced by the formal BUFR (Binary Universal Form for the Representation of meteorological data) format whenever becomes available. The raw data product is collected for 6-hourly time windows centred at synoptic times (00, 06, 12 and 18 UTC).

The data are then averaged along the track to form super-observations with scales compatible with the model scales of around 75 km. It is worthwhile mentioning that the model scale is typically several (4~8) model grid spacing (e.g. Abdalla et al., 2013). This corresponds to 11 individual (1 Hz) Sentinel-3 observations (7 km each).

To achieve this, the stream of altimeter data is split into short observation sequences each consisting of 11 individual (1-Hz) observations. A quality control procedure is performed on each short sequence. Erratic and suspicious individual observations are removed and the remaining data in each sequence are averaged to form a representative super-observation, providing that the sequence has enough number of “good” individual observations (at least 7). The super-observations are collocated with the model and the in-situ (if applicable) data. The raw altimeter data that pass the quality control and the collocated model data are then investigated to derive the conclusions regarding the data quality. The details of the method used for data processing, which is an extension to the method used for ERS-2 RA analysis and described in Abdalla and Hersbach (2004), are presented in Appendix A.

The data are closely monitored and verified using the ECMWF IFS model products. Similar products from other altimeter missions are also used for verification. On a weekly and a monthly basis, the data are verified against available in-situ data in addition to the model data. Internal weekly and monthly plots summarising the quality of Sentinel-3 products for that week or month are also produced, examined and archived for future reference.

This specific report gives the assessment of Level 2 S3A_SR_2_WAT wind and wave products made available by ESA/EUMETSAT through EUMETSAT ODA System covering Sentinel-3A Cycle No. 045 covering the period from 17/05/2019 to 13/06/2019 and Sentinel-3B Cycle No. 026 covering the period from 27/05/2019 to 23/06/2019. Note that several plots show results of Sentinel-3A for the same period of Sentinel-3B Cycle No. 026 (27/05/2019 to 23/06/2019) and therefore, a 10-day shifted-ahead Sentinel-3A cycle is referred to here as Cycle 045+10.

4 Radar Backscatter and Surface Wind Speed

4.1 Backscatter

The Ku-band normalised backscatter coefficient (σ°, Sigma-0 or just backscatter) from Sentinel-3A and Sentinel-3B S3x_SR_2_WAT (x=A or B) product seems to be reasonable and compares very well with that from other altimeters. The backscatter histograms (or the probability density functions, PDF's) of Sentinel-3A and Sentinel-3B SRAL over the global ice-free oceans for the period from 27/05/2019 to 23/06/2019 which corresponds to Cycle 026 of Sentinel-3B and a 10-day shifted-ahead Cycle 045 of Sentinel-3A (will be called here as Cycle 045+10) are shown in Figure 1. The PDF's for Sentinel-3A and 3B are very similar to each other and both are not much different from those of previous cycles (of Sentinel-3B) since the implementation of Sentinel-3A Processing Baseline (PB) version 2.24 and Sentinel-3B PB version 1.13. Sentinel-3 backscatter PDF compares quite well with those of other Ku-band altimeters (after adjusting Jason-2/3 backscatter by about 2.5 dB; not shown).

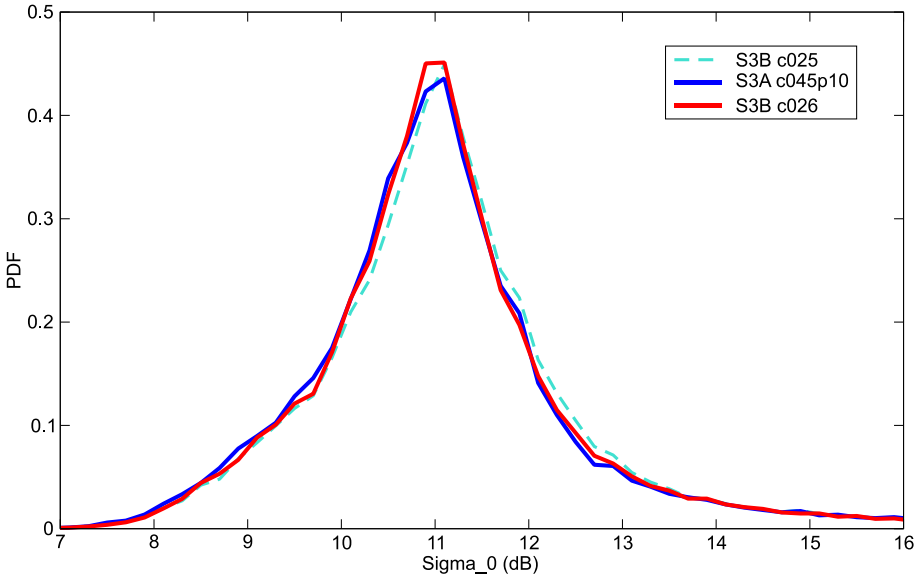

Figure 1: Sentinel-3A SRAL ocean Ku-band backscatter histogram (PDF) over the whole globe and for the period from 27/05/2019 to 23/06/2019 which corresponds to Cycle 026 of Sentinel-3B and a 10-day shifted-ahead Cycle 045 (045+10) of Sentinel-3A. For comparison, the same plot from the previous Sentinel-3B cycle is also shown.

The time series of the global (ice-free ocean only) mean and standard deviation (SD) of backscatter coefficients from SRAL of both Sentinel-3A and 3B are shown in Figure 2. To emphasise the long-term changes, 92-day running means are also shown. The temporal change in the mean and the SD of backscatter is not much different than the other altimeters (not shown). The plot shows the average of a moving window of 7 days moved by one day at a time to produce smooth plots. Both the mean and the SD of the backscatter are stable over the last few cycles apart from a slight increase in the mean value of the backscatter after the implementation of PB 2.24. As can be seen in Figure 2 the mean backscatter reached the highest value in early April 2018 (end of Sentinel-3A Cycle 029-A). The change of mean and

standard deviation of the backscatter after the implementation of PB 2.27 on 14 February 2018 are within their usual variability. **There has been a linearly increasing trend of the global mean of the backscatter coefficient since the end of 2017. However, this increasing trend tends to become smaller before changing into a decreasing trend between the end of September and the end of December 2018. It started to increase again since end of December 2018. This is a strong indication of a seasonal signal.**

Since the implementation of Sentinel-3B PB 1.13 on 6 December 2018, the global mean ocean backscatter values from Sentinel-3A and Sentinel-3B are very close with **Sentinel-3B value is higher by about 0.1 dB**. The standard deviation of the backscatter from both satellites was almost identical during the tandem phase. After that, there are some minor differences which is normal considering that both altimeters do not sample the global ocean at the same time.

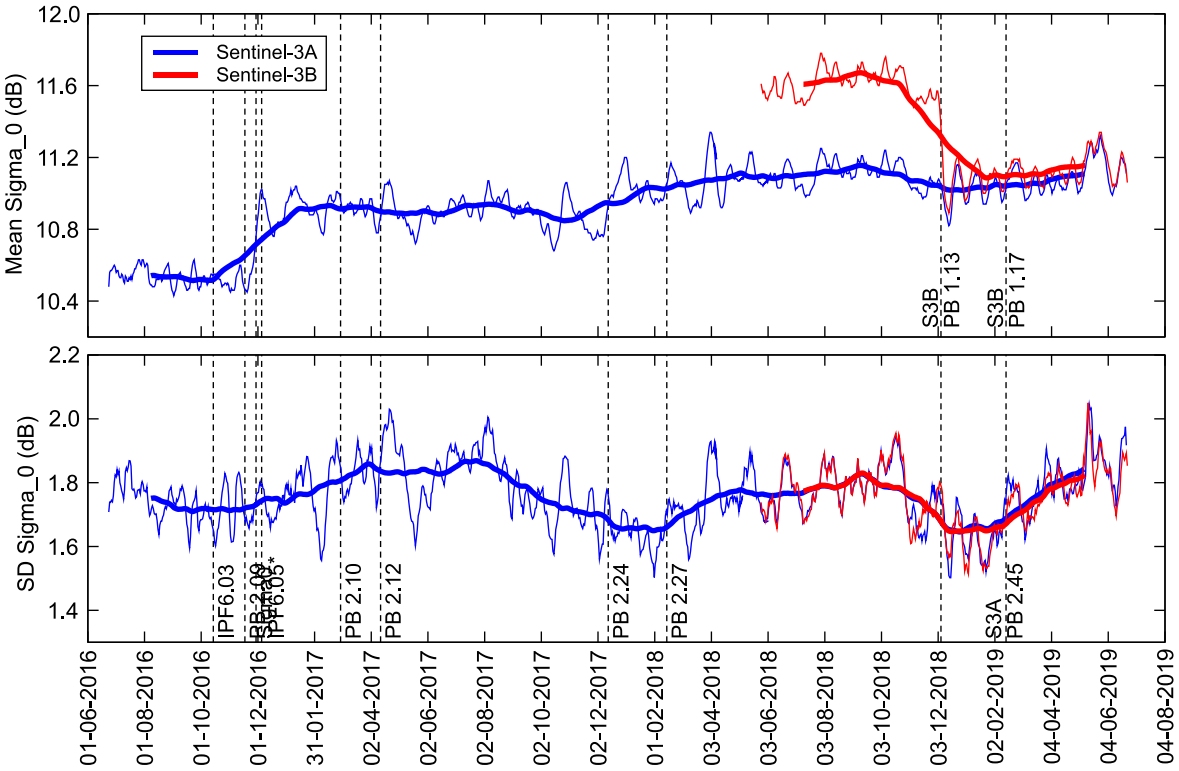

Figure 2: Time series of global mean (top) and standard deviation (bottom) of backscatter coefficient of SRAL Ku-band from both Sentinel-3A and Sentinel-3B after quality control. Mean and SD are computed over a moving time window of 7 days and are shown as thin lines. The 92-day running means are shown as thick lines.

4.2 SAR Mode Surface Wind Speed

Figure 3 shows the global SAR wind speed PDF's of Sentinel-3A for Cycle 045+10 (Cycle 045 shifted ahead by 10 days to cover the same period as that of Sentinel-3B Cycle 026) and of Sentinel-3B for Cycle 026. The PDF of the previous Sentinel-3B cycle is shown for comparison. The PDF's of the corresponding ECMWF Integrated Forecast System (IFS) model wind speed collocated with Sentinel-3 during the same cycles are also shown. The PDF's of Sentinel-3A and 3B wind speed are close to those of the model (as

well as the other altimeters; not shown). However, there are few deviations mainly around the peak of the PDF. The difference between the PDF's of both altimeters is mainly due to geographical sampling since a common period is utilised.

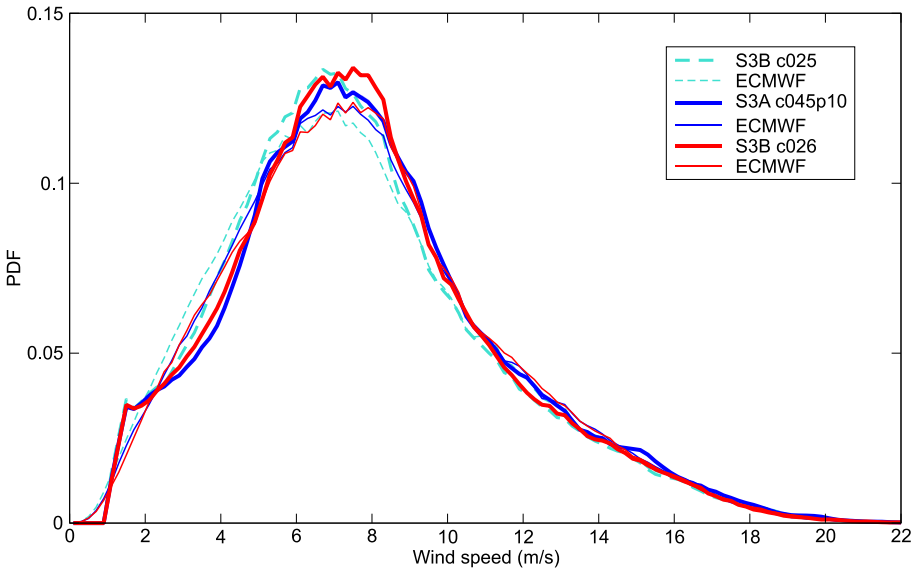

Figure 3: Sentinel-3 SRAL SAR surface wind speed PDF's over the whole global ocean and for the period from 27/05/2019 to 23/06/2019 which corresponds to Cycle 026 of Sentinel-3B and a 10-day shifted-ahead Cycle 045 (045+10) of Sentinel-3A. The corresponding ECMWF (collocated with Sentinel-3) PDF's are also shown for comparison. The corresponding PDF's (SRAL and model) from the previous Sentinel-3B cycle are also shown as dashed lines.

Collocated pairs of altimeter super-observation and the analysed (AN) ECMWF model wind speeds are plotted in a form of a density scatter plot in Figure 4 for the whole global ocean over the period from 27/05/2019 to 23/06/2019 which corresponds to Sentinel-3A Cycle 045+10 in panel (a) and to Sentinel-3B Cycle 026 in panel (b). The scatter plots in Figure 4 and other similar wind speed scatter plots that appear hereafter represent two-dimensional (2-D) histograms showing the number of observations in each 2-D bin of 0.5 m/s $\times$ 0.5 m/s of wind speed. The agreement between Sentinel-3 winds and their model counterpart is very good with virtually no bias (around 0.1 m/s for Sentinel-3A and around -0.1 m/s for Sentinel-3B). SAR wind speed products from both altimeters are as good as (if not slightly better than) their counterparts from the other altimeters. The standard deviation of the difference (SDD) with respect to the model, which can be used as a proxy for the random error, is about 1.09 and 1.08 m/s for Sentinel-3A and Sentinel-3B, respectively (about 14.0% of the mean for both) which is similar to (or even slightly better than) that of other altimeters. The other fitting statistics are shown in the offset of the two panels of Figure 4.

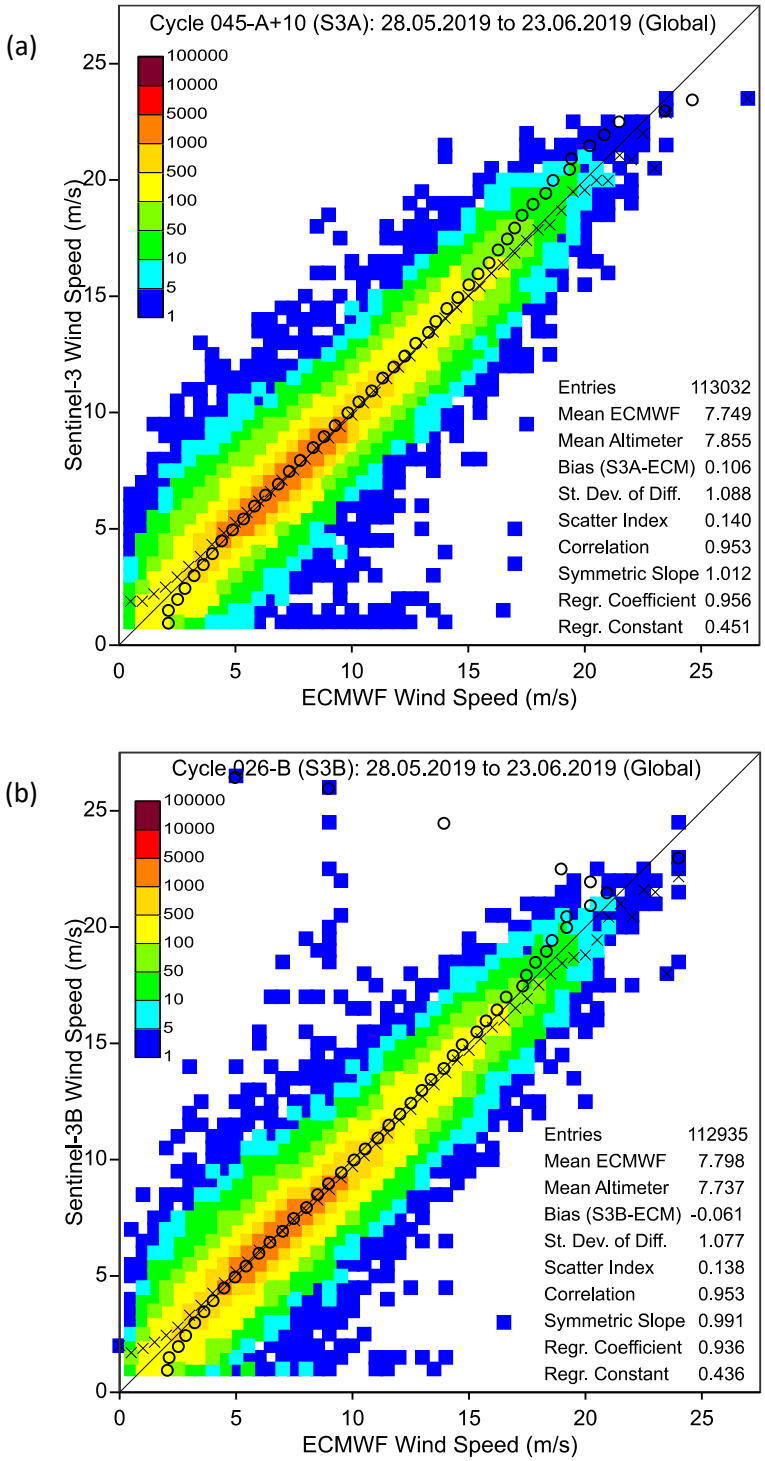

Figure 4: Global comparison between Sentinel-3 SRAL and ECMWF model analysis surface wind speed values over the period from 27/05/2019 to 23/06/2019 which corresponds to a 10-day shifted-ahead Cycle 045 (045+10) of Sentinel-3A (a) and Sentinel-3B Cycle 026 (b). The number of collocations in each 0.5 m/s x 0.5 m/s 2D bin is color-coded as in the legend. The crosses are the means of the bins for given x-axis values (model) while the circles are the means for given y-axis values (Sentinel-3).

The scatter plots for Sentinel-3 SAR wind speed versus the model collocations discriminated based on their geographical locations whether in the Northern Hemisphere (north of latitude 20°N; NH), the Tropics (between latitudes 20°S and 20°N) or the Southern Hemisphere (south of latitude 20°S; SH) are shown in panels (a), (b) and (c) of Figure 5, respectively, for Sentinel-3A and in panels (d), (e) and (f), respectively, for Sentinel-3B. Corresponding plots from both satellites compare very well with each other. Compared to the similar plots from previous cycles for Sentinel-3A, one can notice a seasonal cycle in the bias behaviour of SRAL SAR mode compared to the model within the range from 7 to 15 m/s with slight overestimation in NH and slight underestimation in the SH during June to August and vice versa during November to March. Further monitoring and analysis are needed to confirm this and provide a possible explanation.

The time series of the global mean and standard deviation (SD) of the wind speed from Sentinel-3A and Sentinel-3B over a 7-day time window moving by 1 day at a time are shown in the upper and lower panels, respectively, of Figure 6. The corresponding time series of the model collocated with Sentinel-3A are also shown for comparison. The time series of model collocated with Sentinel-3B are not different from the shown ones. To emphasise the long-term changes, 92-day running means are also shown.

It is clear from Figure 6 that since 6 December 2016 Sentinel-3A mean wind speed is very close to that of the model. The global standard deviation of the altimeter measurements has been slightly lower than that of the model except for the months of July and August 2017 when both global standard deviation values were almost equal. This could not be correlated to any of the processing or model changes (see Section 2). The same happened during July and August 2018 (compare the 92-day running means) suggesting that this is due to geophysical seasonal effects. Figure 6 does not suggest that PB 2.24 and PB 2.27 have any impact on wind speed mean and SD. **The increasing trend in the Sentinel-3A backscatter global mean is reflected as a small decreasing trend in the wind speed global mean between the end of 2017 and September 2018. This trend was reversed from September to December 2018 (when the trend in backscatter was reversed). Since the end of 2018, irrespective of the slight increasing trend in backscatter coefficient, there is no clear sign of any trend.**

Since 6 December 2018 when Sentinel-3B PB 1.13 was implemented, Sentinel-3B wind speed Sentinel-3B wind speed compares very well with that of Sentinel-3A and that of the model both in terms of the global mean and the global standard deviation as can be seen in Figure 6b. Note that Sentinel-3B mean wind is closer to the model mean than that of Sentinel-3A. **The latter is higher by about 0.15 m/s which is a relatively small difference. Sentinel-3B SD of wind speed is the lowest.**

The time series of the wind speed weekly bias (defined as the altimeter – model) and standard deviation of the difference (SDD) of Sentinel-3A SRAL compared to the ECMWF model AN are shown in the upper and lower panels, respectively, of Figure 7. Since the implementation of PB 2.09 (including the adjustment of sigma_0) in early December 2016, there is virtually no bias between Sentinel-3A and model winds. Although the global bias is almost zero, there are small regional biases within ±0.5 m/s. The wind speed bias in each hemisphere follows a seasonal pattern. The bias has its minimum during the hemispheric summer while its maximum is attained during the hemispheric winter. The SH bias pattern is off-phase with respect to the NH pattern with smaller amplitude. The bias in the Tropics is constant at about 0.1 m/s.

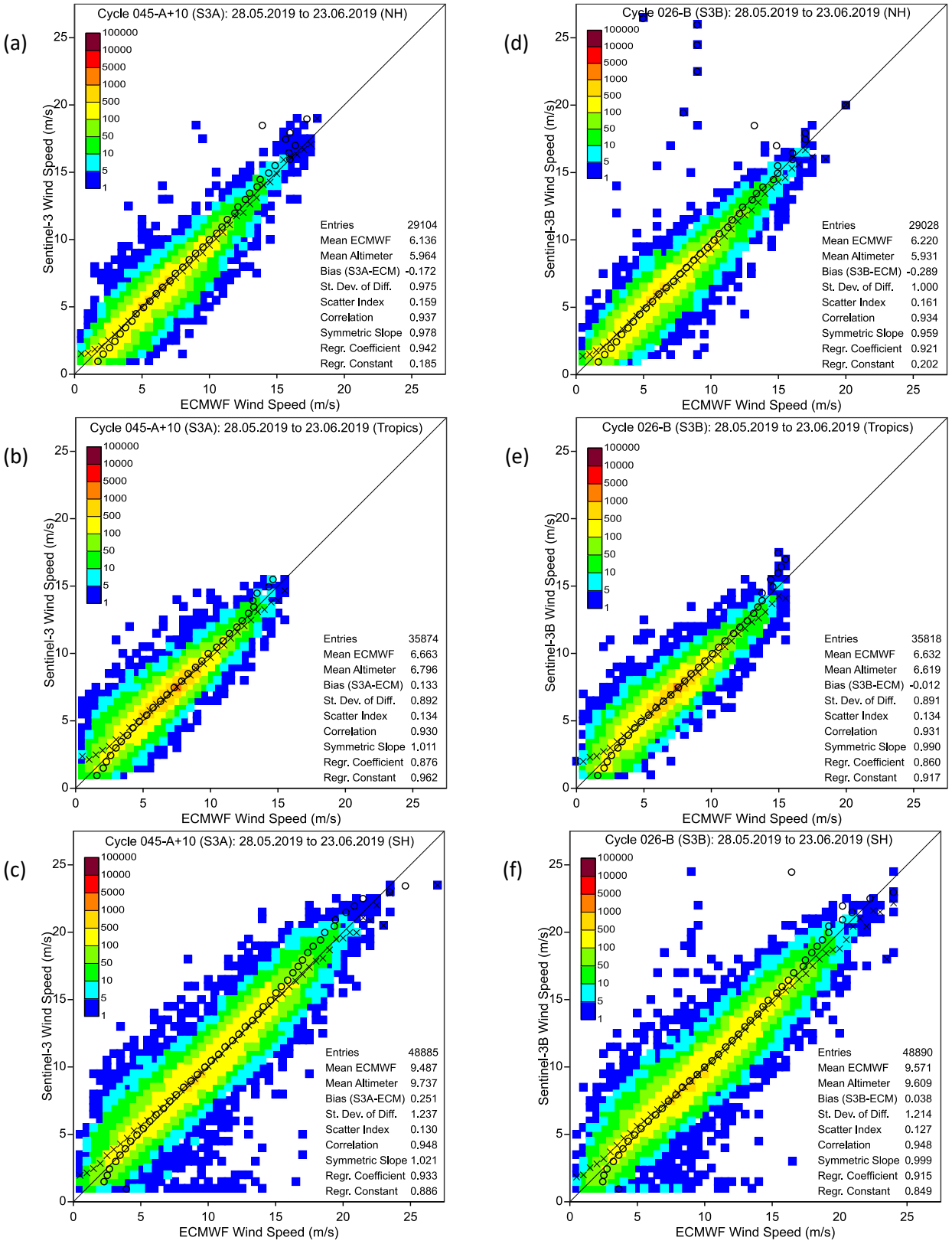

Figure 5: Same as Figure 4 but for Northern Hemisphere (north of 20° N), Tropics (20° S - 20° N) and Southern Hemisphere (south of 20° S), respectively. Sentinel-3A plots on the left-hand side while S-3B plots on the right.

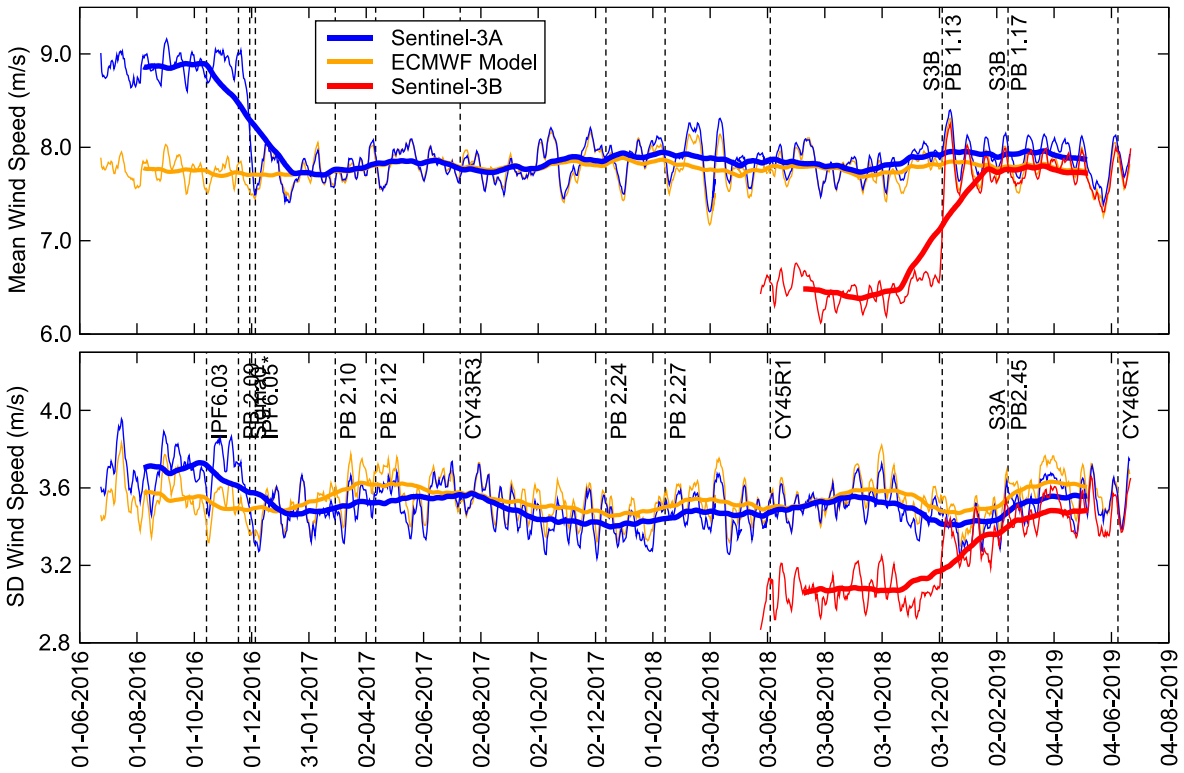

Figure 6: Time series of global mean (top) and standard deviation (bottom) of wind speed from SRAL Ku-band after quality control from both Sentinel-3A and Sentinel-3B. The collocated model wind speed mean and SD are also shown. Mean and SD are computed over a moving time window of 7 days (shown as thin lines). The 92-day running means are shown as thick lines.

Figure 7 also shows that since early December 2016 (implementation of PB 2.09), Sentinel-3A global wind speed SDD values with respect to the model have been fluctuating between 1.0 and 1.2 m/s which is slightly smaller than the corresponding values from other altimeters (not shown). The extra-tropics hemispherical SDD values follow a seasonal cycle in phase of the cycle observed in the bias plots (peaks down during the summer of the hemisphere and peaks up during the winter period).

The time series of the wind speed weekly bias and SDD of Sentinel-3B compared to the ECMWF model AN are shown in the upper and lower panels, respectively, of Figure 8. Since 6 December 2018 with the implementation of Sentinel-3B PB 1.13, Sentinel-3B winds have been virtually unbiased with lower SDD values compared to the model. Sentinel-3B wind speed bias and SDD are very close to those of Sentinel-3A (about zero bias and slightly above 1 m/s SDD).

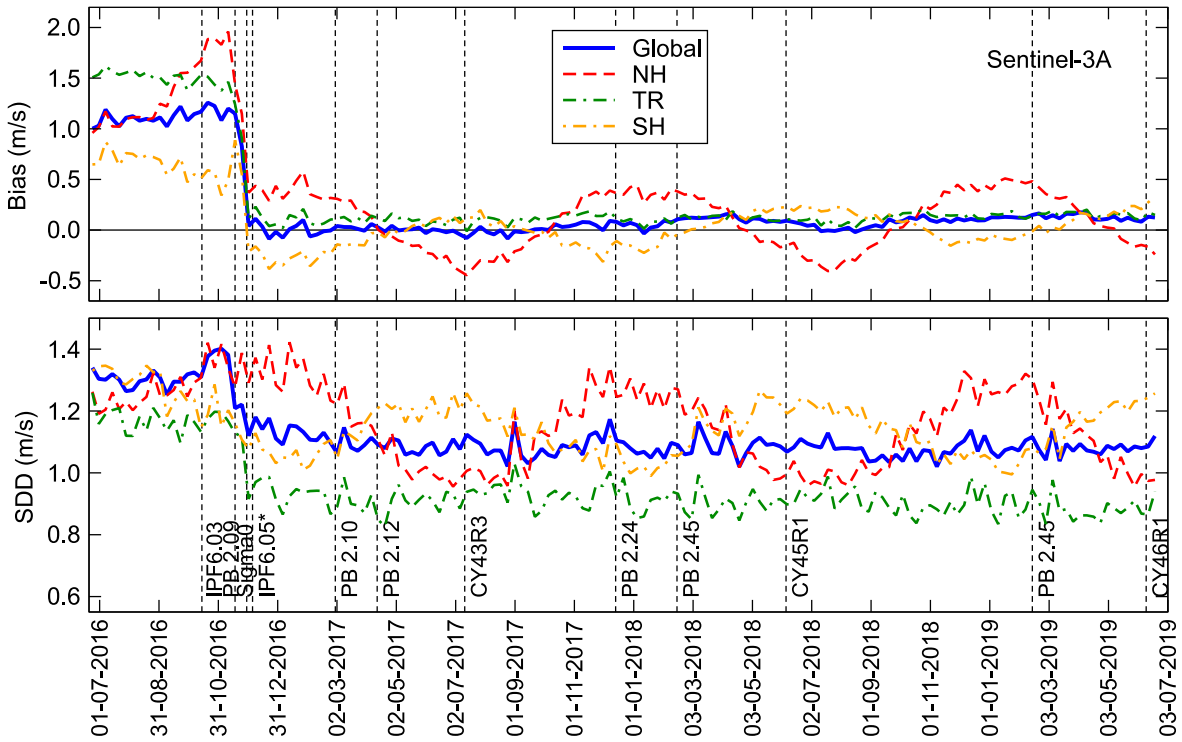

Figure 7: Time series of weekly wind speed bias defined as altimeter - model (top) and standard deviation of the difference (bottom) between Sentinel-3A SRAL Ku-band and ECMWF model analysis.

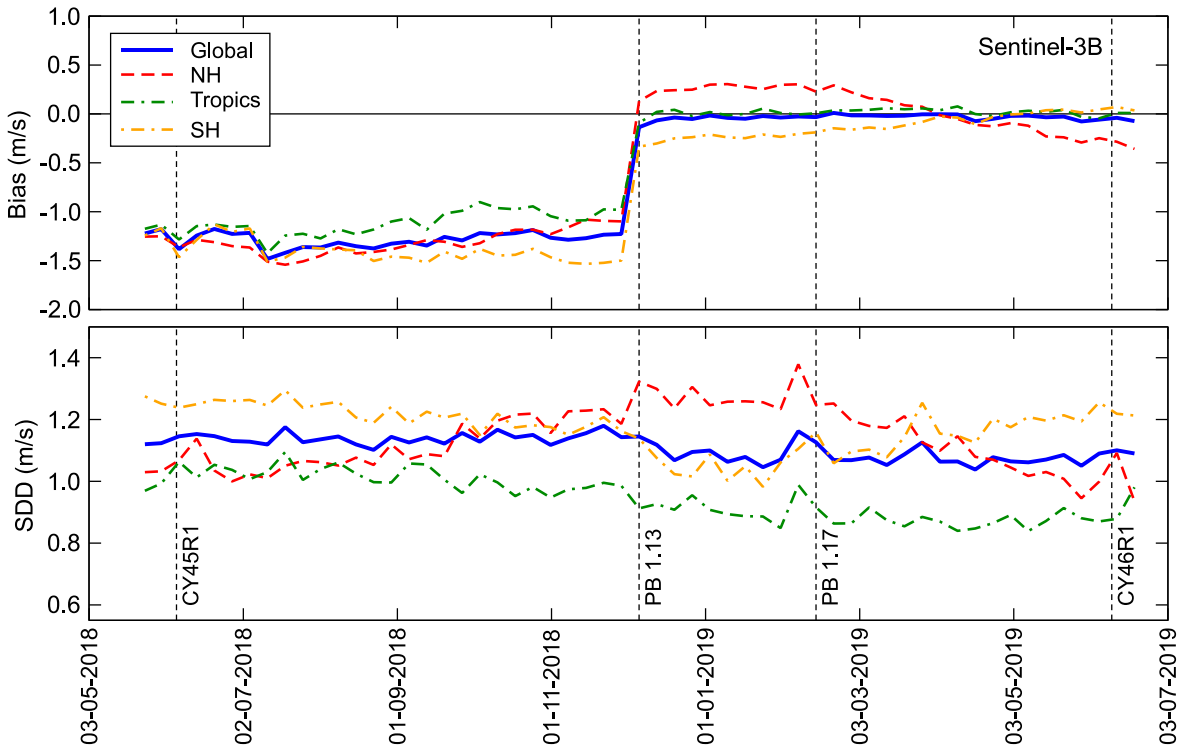

Figure 8: Same as Figure 7 but for Sentinel-3B.

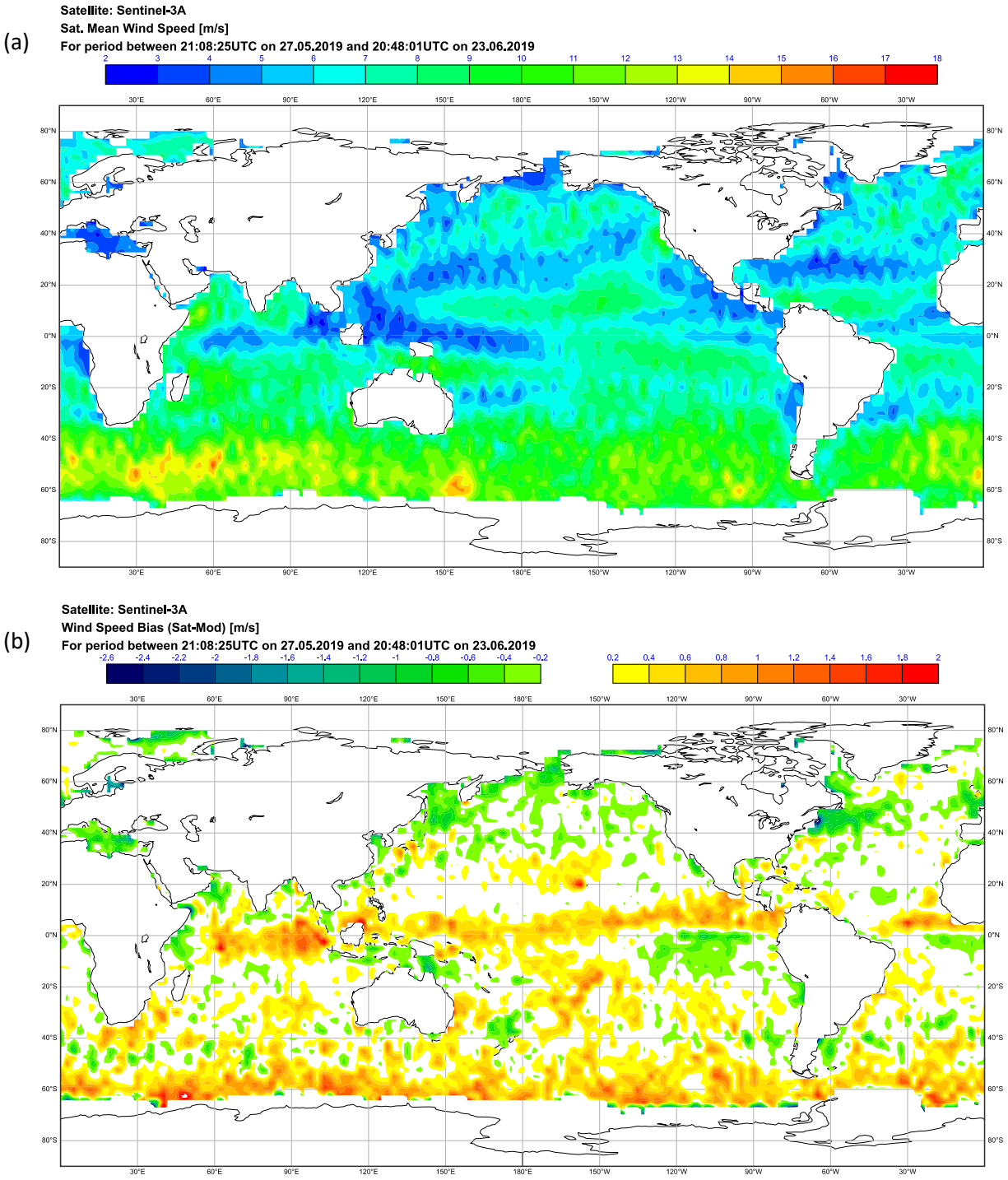

Figure 9: Geographical distribution of mean Sentinel-3A wind speed (a) as well as the bias (b); the SDD (c) and the SI (d) between Sentinel-3A and ECMWF model AN during the period from 27/05/2019 to 23/06/2019 which corresponds to a 10-day shifted-ahead Cycle 045 (045+10) of Sentinel-3A. Bias is defined as altimeter – model.

(c)

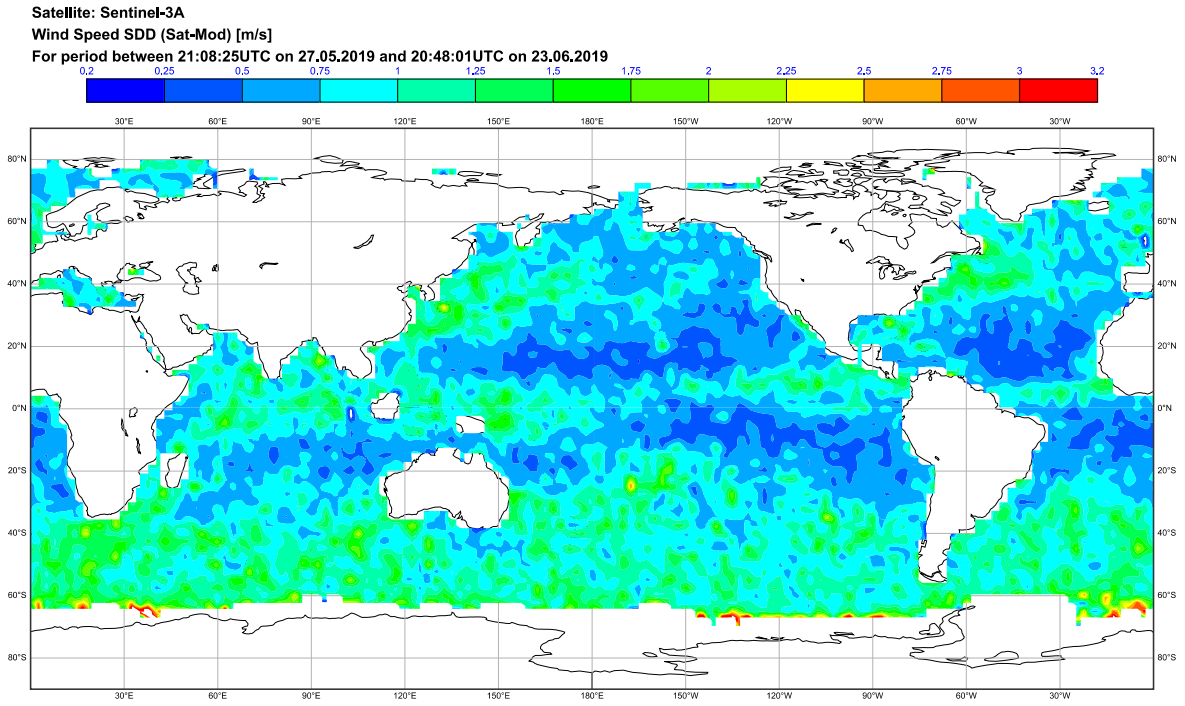

(d)

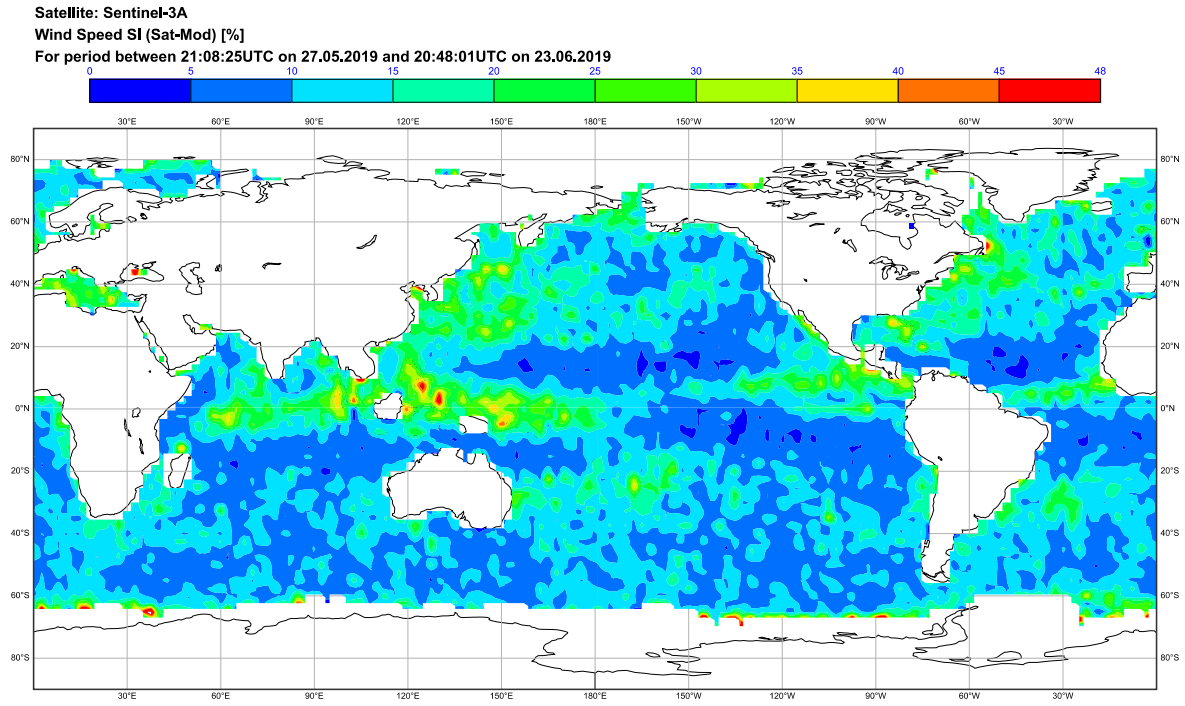

Figure 9: Continued.

(a)

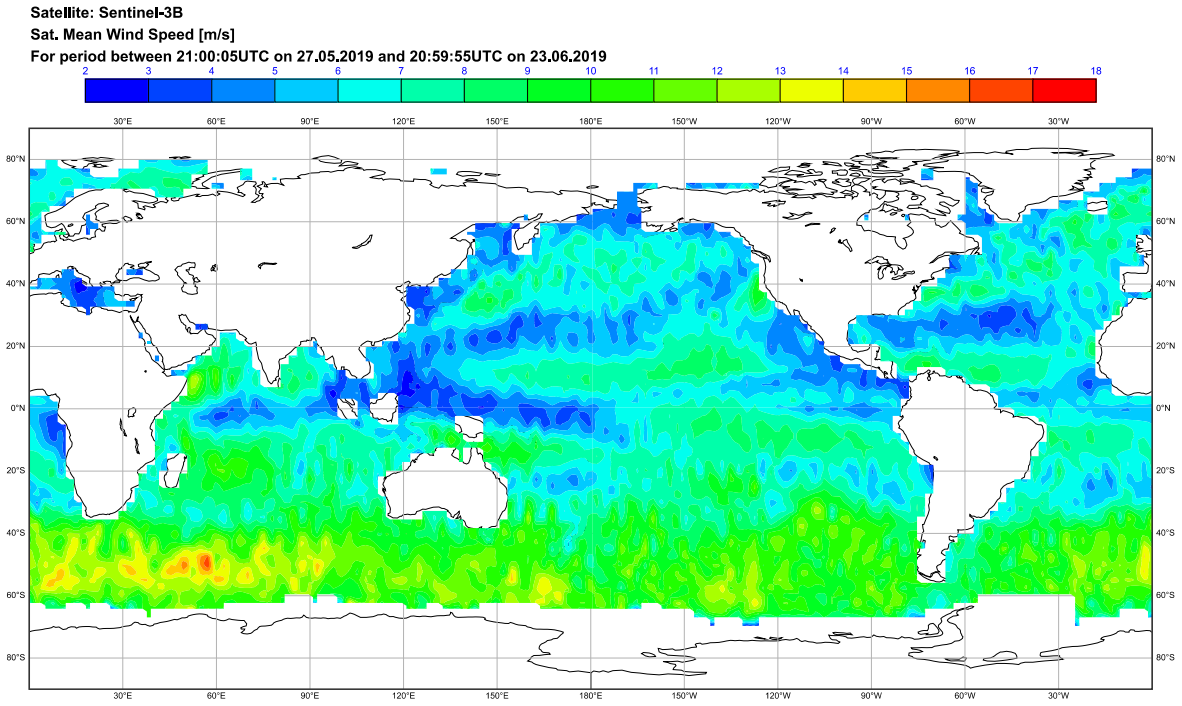

(b)

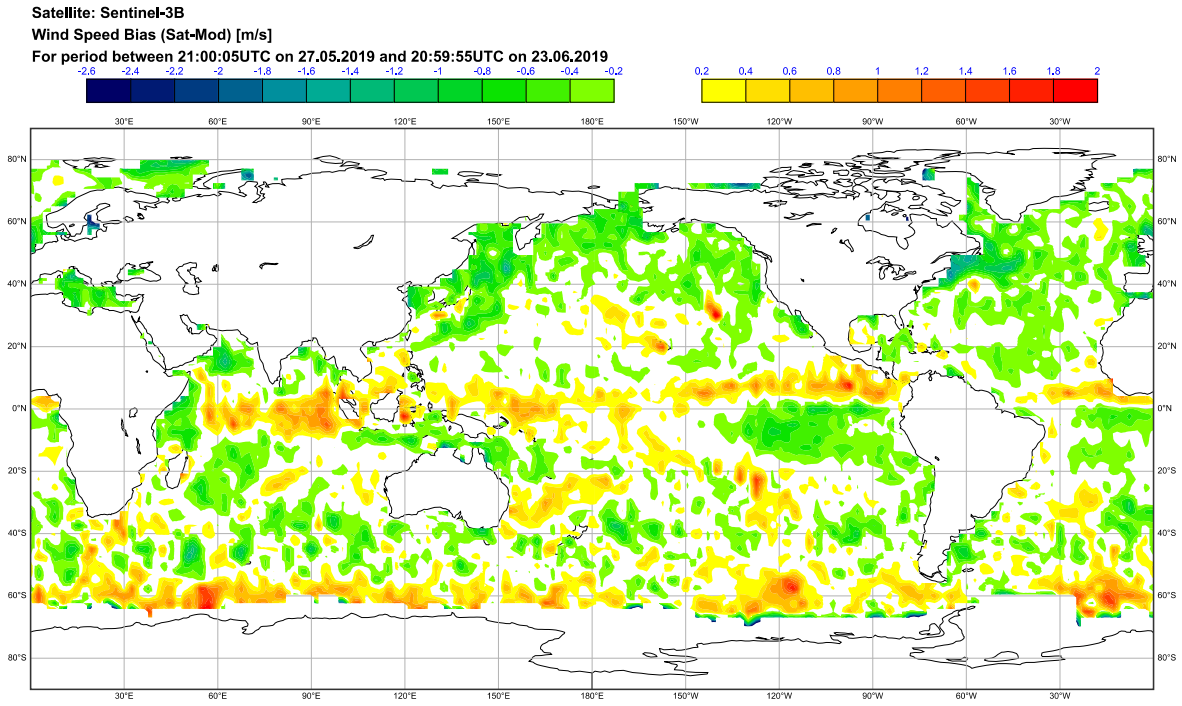

Figure 10: Same as Figure 9 but for Sentinel-3B Cycle 026 from 27/05/2019 to 23/06/2019.

(c)

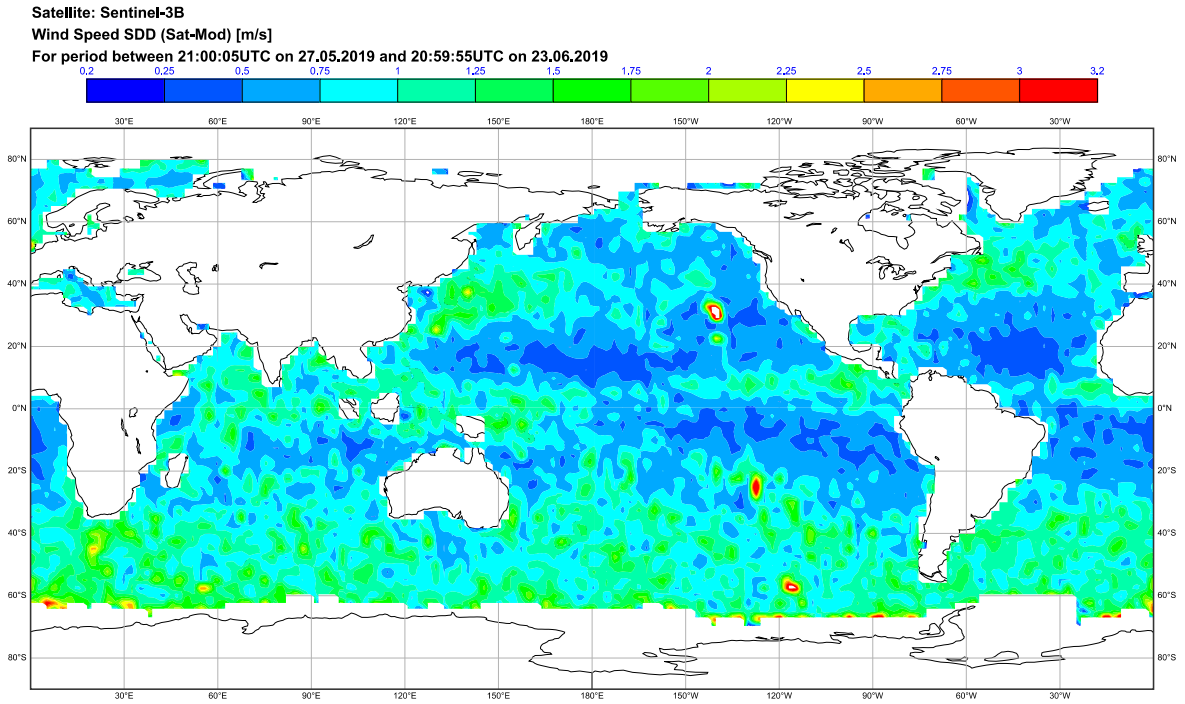

(d)

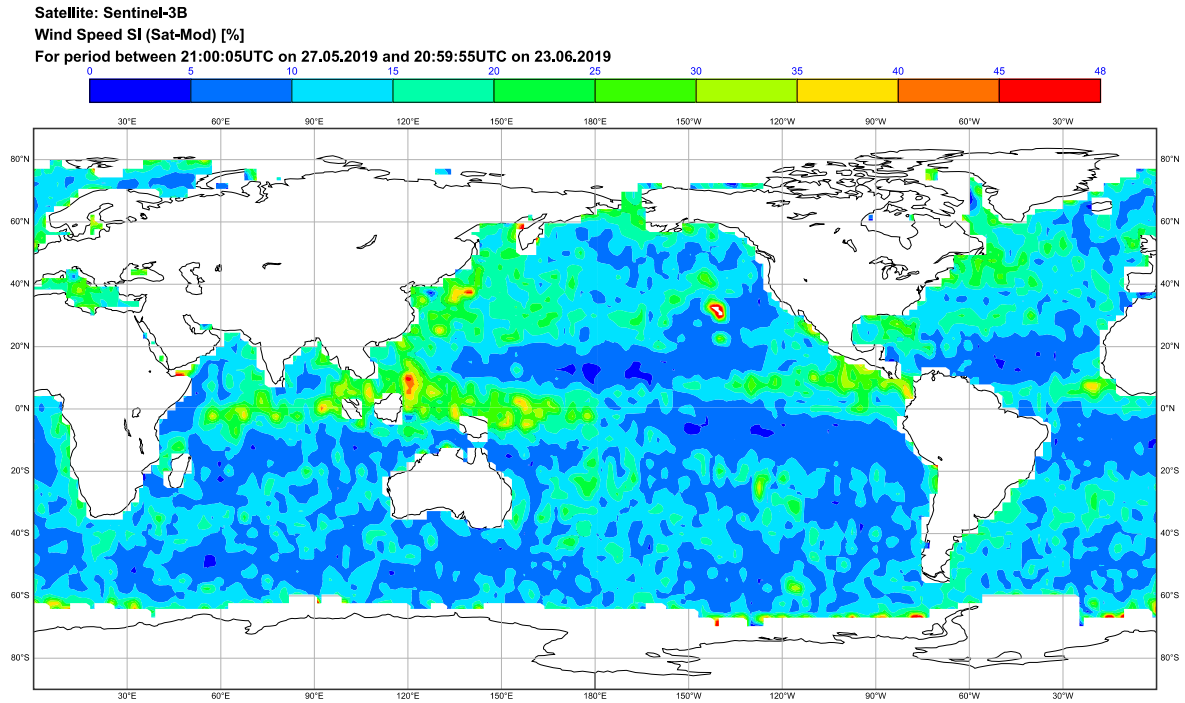

Figure 10: Continued.

Figure 6 and Figure 7 do not show any impact that might be caused by the implementation of Sentinel-3A PB 2.10 which was introduced on 28 February 2017. However, the positive impact is clear when the SDD between SRAL and ECMWF model is compared to SDD values of other altimeters. On the other hand, PB 2.24 and PB 2.27 do not seem to have any impact on the bias and the SDD between SAR and model wind speeds according to Figure 7. However, comparison with respect to the same plots from

other altimeters (not shown here but can be found in the 2017 annual report), suggests that PB 2.24 may be responsible for a minor improvement in Sentinel-3A SAR winds.

The impact of the processing chains Sentinel-3A PB 2.45 and Sentinel-3B PB1.17, implemented operationally on 14 February 2019, is neutral.

The geographical distribution of the mean Sentinel-3A wind speed and the wind speed bias, SDD and scatter index (SI, defined as the SDD divided by the model mean and expressed in percentage in the last panel) with respect to the ECMWF model averaged over the period of Cycle 045+10 are shown in Figure 9. The corresponding maps from Sentinel-3B Cycle 026 are shown in Figure 10. While the mean wind speed, the SDD and SI distributions all look similar to their counterparts from other altimeters (not shown), the bias in panel (b) of both Figure 9 (Sentinel-3A) and Figure 10 (Sentinel-3B) is rather low almost everywhere.

The comparison against in-situ (mainly buoys located in the Northern Hemisphere around the American and European coasts) measurements is shown in panels (a) and (b) Figure 11 for Cycle 045+10 (Sentinel-3A) and Cycle 026 (Sentinel-3B), respectively. The overall bias values against in-situ observation for Sentinel-3A and Sentinel-3B are about -0.5 and -0.6 m/s, respectively. The SDD (a proxy to the random error) values are around 1.1 m/s and 1.3 m/s for Sentinel-3A and Sentinel-3B, respectively, which are about 17% of the mean for both altimeters. These values are similar to the corresponding statistics emerging from the comparison of other altimeters against in-situ observations (not shown).

4.3 PLRM Surface Wind Speed

Collocated pairs of SRAL Pseudo Low Rate Mode (PLRM) wind speed super-observation and the analysed (AN) ECMWF model wind speeds are plotted as density scatter plots over the whole globe for the period from 27/05/2019 to 23/06/2019 which corresponds to Sentinel-3A Cycle 045+10 in panel (a) and to Sentinel-3B Cycle 026 in panel (b) of Figure 12. Obviously, the agreement between PLRM winds from both altimeters and their model counterpart is very good.

There is a number obviously wrong zero PLRM wind speed values (see, for example, the cyclic report of Cycle 012-A) which could not be filtered out using the quality control described in the appendix. In order to remove the distraction of those outliers they were eliminated using a small threshold.

The PLRM wind from both satellites is globally unbiased (bias of not more than 0.2 m/s) when compared to the model. The standard deviation of the difference is about **1.4 m/s (~17% of the mean)**. These SDD values are slightly higher that the corresponding values of the last few cycles **(needs to be verified)** but similar to their counterparts from other altimeters. The scatter plots for Sentinel-3A PLRM wind versus the model collocations discriminated based on their geographical locations whether they are in the Northern Hemisphere (north of latitude 20°N), the Tropics (between latitudes 20°S and 20°N) or the Southern Hemisphere (south of latitude 20°S) are shown in panels (a), (b) and (c) of Figure 13, respectively, for Sentinel-3A and in panels (d), (e) and (f), respectively, for Sentinel-3B. Sentinel-3A bias follows a seasonal pattern in both hemispheres as was noticed for the SAR wind speed. However, unlike the SAR wind there is no clear seasonality in the SDD for the PLRM wind.

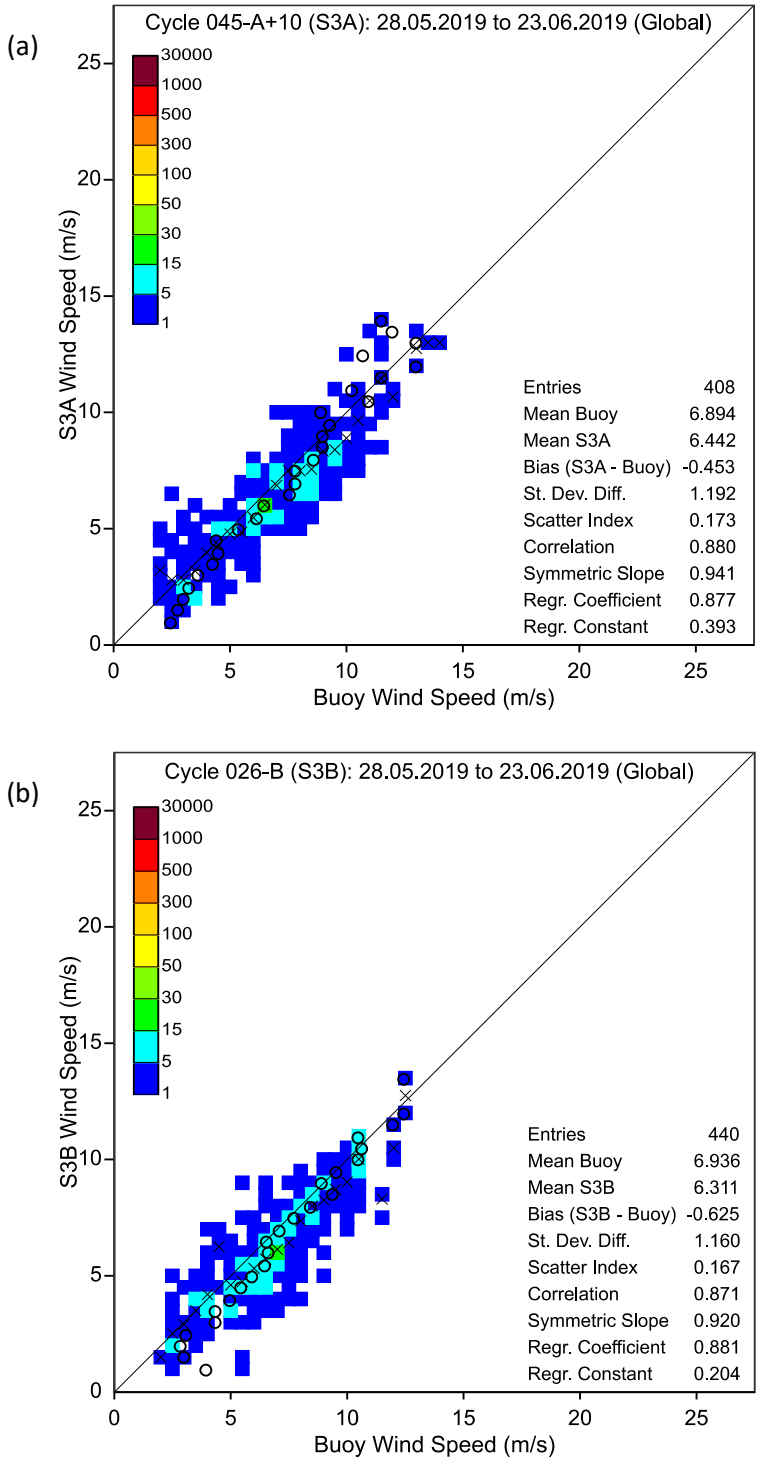

Figure 11: Same as Figure 4 but the comparison is done against in-situ observations (mainly in the NH).

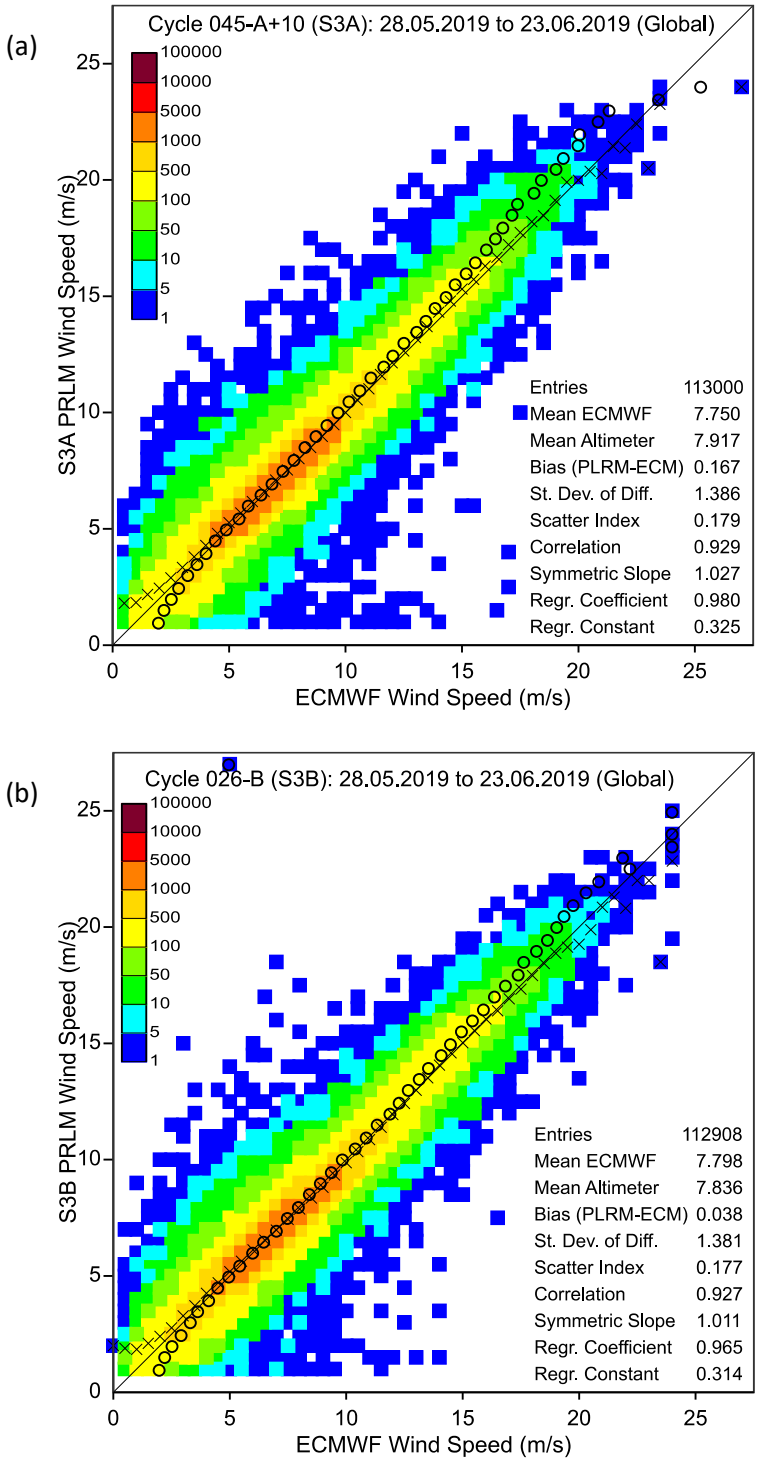

Figure 12: Global comparison between Sentinel-3 PLRM and ECMWF model analysis wind speed values over the period from 27/05/2019 to 23/06/2019 which corresponds to a 10-day shifted-ahead Cycle 045 (045+10) of Sentinel-3A (a) and Sentinel-3B Cycle 026 (b). Refer to Figure 4 for the meaning of the crosses and the circles as well as the colour coding.

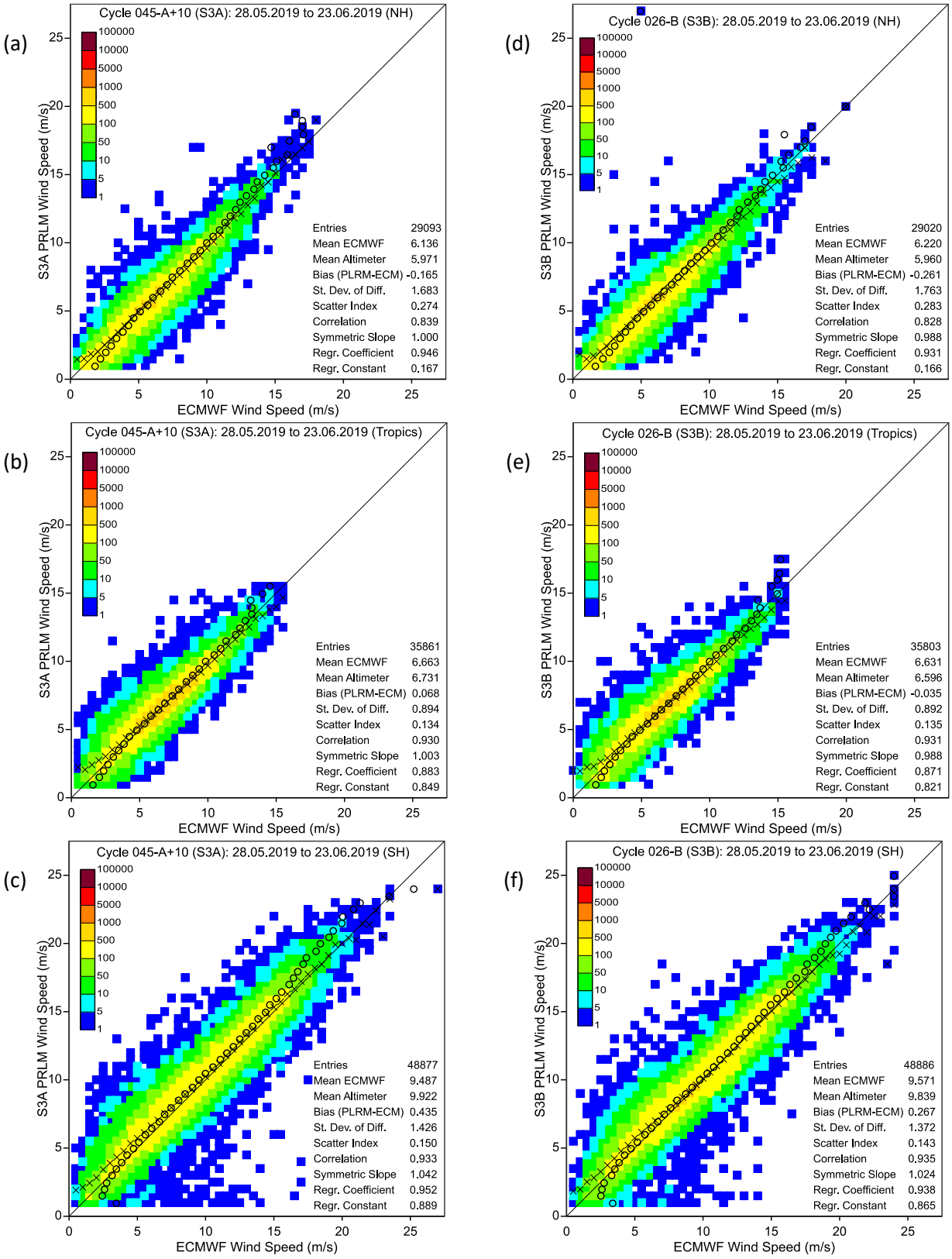

Figure 13: Same as Figure 12 but for (a) Northern Hemisphere (north of 20°N), (b) Tropics (20°S - 20°N) and (c) Southern Hemisphere (south of 20°S), respectively. Sentinel-3A plots on left-hand side while 3B plots on right.

The time series of the weekly bias and the SDD between PLRM wind speed and that of the model are shown in Figure 14 and Figure 15 for Sentinel-3A and Sentinel-3B, respectively. Since early December 2016 (implementation of Sentinel-3A PB 2.09), Sentinel-3A wind speed has been globally unbiased with respect to the model winds.

The SDD between Sentinel-3A and the model for the last few cycles is the lowest ever (less than 1.1 m/s). Before that, SDD plateaued at about 1.2-1.4 m/s. However, there has been few short periods with high SDD values that exceeded 1.4 m/s especially in the NH between mid-June and early September 2017 in addition to a recent one at the beginning of April 2018. Similar high SDD values appeared again from mid-June till early September 2018.

The processing changes of PB 2.24 and PB 2.27 do not seem to have any impact on PLRM wind speed.

There has been a clear drop in the SDD between PLRM wind and the model since early September 2018. For the time being there is no explanation for that drop which could be artificial.

The impact of the processing chains Sentinel-3A PB 2.45 and Sentinel-3B PB1.17, implemented operationally on 14 February 2019, is neutral.

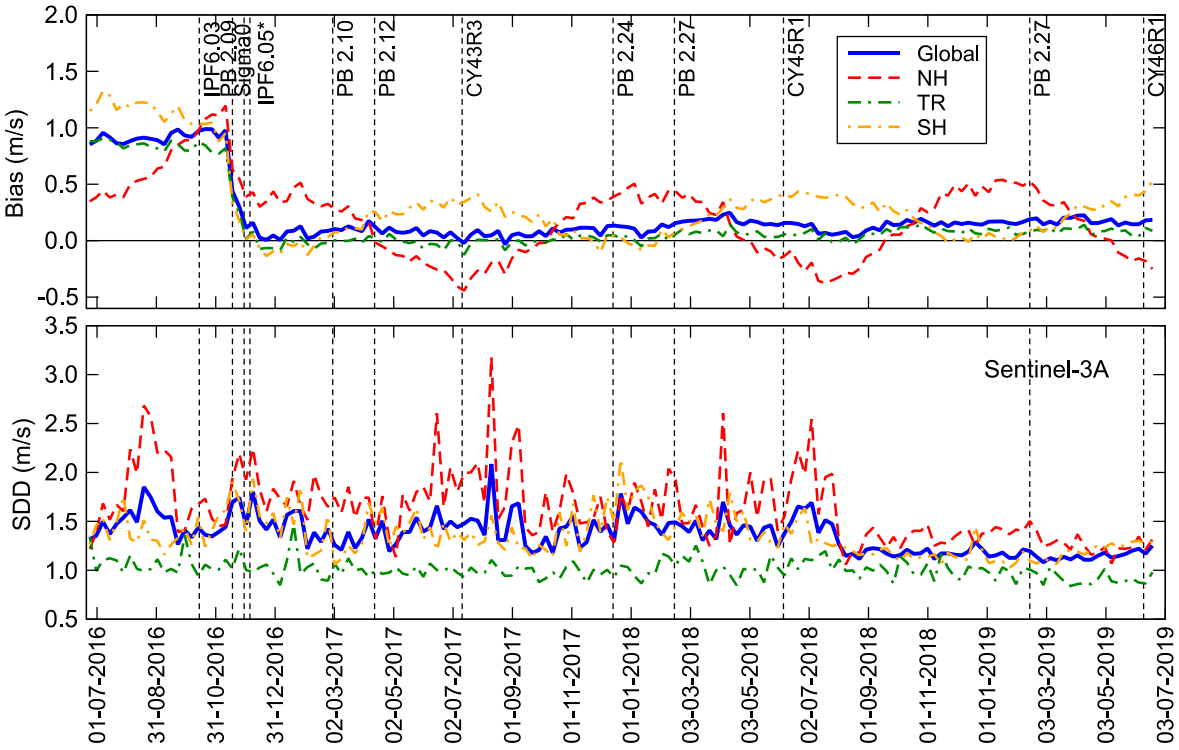

Figure 14: Time series of weekly PLRM wind speed bias defined as altimeter - model (top) and standard deviation of the difference (bottom) between Sentinel-3A SRAL PLRM and ECMWF model analysis.

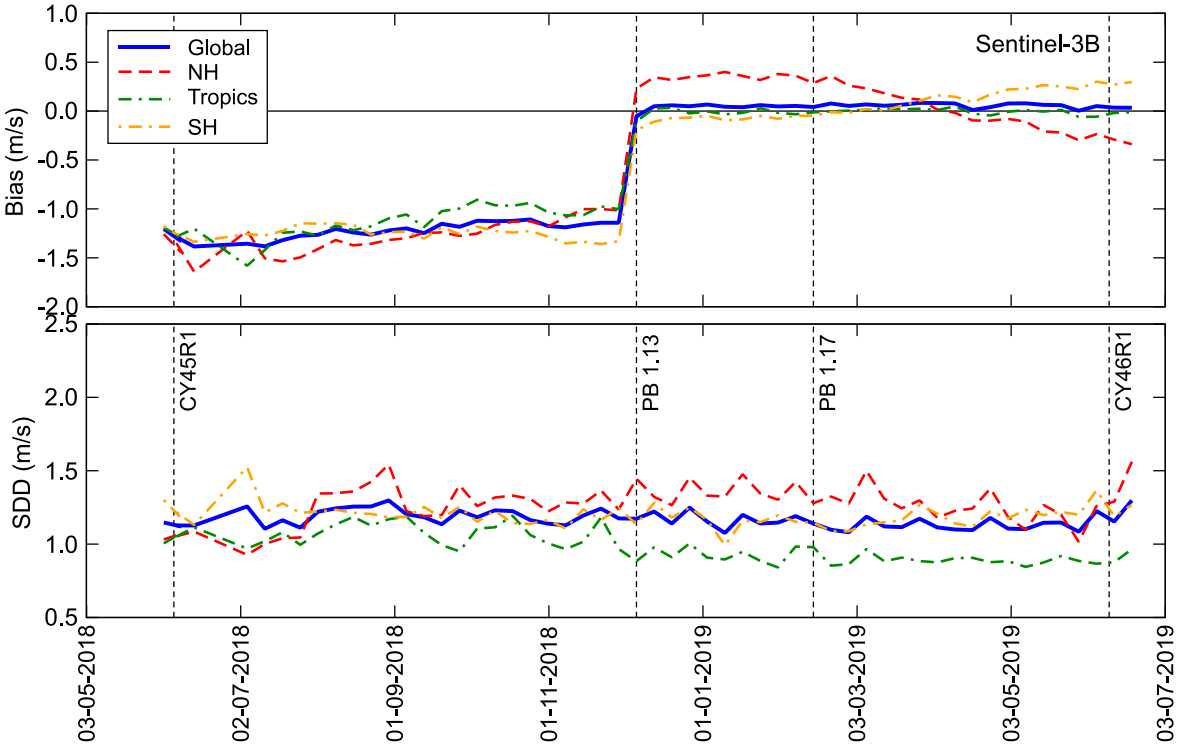

Figure 15: Same as Figure 14 but for Sentinel-3B.

5 Significant Wave Height

Altimeter significant wave height (SWH) is the most important product as far as the wave prediction is considered. It is used for data assimilation to improve the model analysis and forecast. Therefore, there is great interest at ECMWF to monitor, validate and assimilate such data products. SWH from available altimeters are assimilated in the ECMWF model. Therefore, the model first-guess (which is practically a model short-forecast) is used for the verification to reduce the impact of error correlation between the model and Sentinel-3 SRAL that may be conveyed through sharing the same principle of measurement with the altimeters whose SWH products are being assimilated.

Figure 16 shows the global SWH PDF's of Sentinel-3A for the period from 27/05/2019 to 23/06/2019 which corresponds to Sentinel-3A Cycle 045+10 and to Sentinel-3B Cycle 026. The PDF's of the previous Sentinel-3B cycle is shown for comparison. The PDF's of the ECMWF Integrated Forecast System (IFS) model SWH collocated with Sentinel-3 for the three cycles are also shown. The SWH PDF's of both Sentinel-3 altimeters deviate slightly from their model counterpart as well as those of other altimeters (not shown). The deviations are mainly around the peak of the PDF (located at around SWH of 2 m). **There is also more than usual number of small SWH values (< 1.0 m) after the implementation of Sentinel-3A PB 2.27. This was confirmed by the analysis of the reprocessed data set that used PB 2.27 and covers more than 18 months. Similar observation can be seen for Sentinel-3B.**

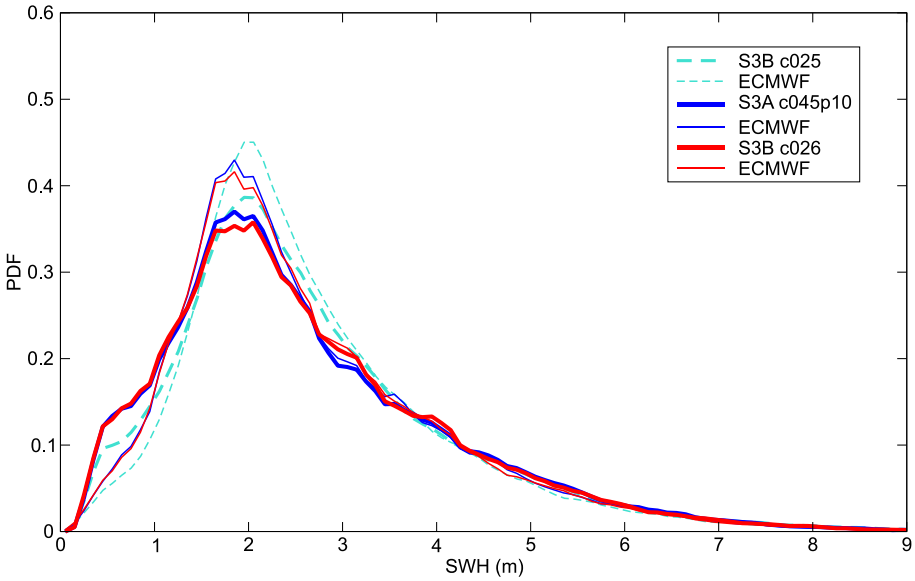

Figure 16: Sentinel-3 SRAL SWH PDF's over the whole global ocean and for the period from 27/05/2019 to 23/06/2019 which corresponds to Cycle 026 of Sentinel-3B and a 10-day shifted-ahead Cycle 045 (045+10) of Sentinel-3A. The corresponding ECMWF (collocated with Sentinel-3) PDF's are also shown for comparison. The corresponding PDF's from the previous Sentinel-3B cycle are shown as dashed lines.

There is a hint of the small secondary peak in the SWH PDF of both altimeters and their model counterpart at SWH of about 3 m, which emerges from time to time in the cyclic PDF's. Although this is probably a geophysical signal, it will be monitored during the coming few cycles.

Collocated pairs of altimeter super-observation and the ECMWF model SWH FG are plotted as density scatter plots over the whole globe for Sentinel-3A over the period from 27/05/2019 to 23/06/2019 which corresponds to a 10-day shifted-ahead Cycle 045 (045+10) of Sentinel-3A and to Cycle 026 of Sentinel-3B in panels (a) and (b), respectively, of Figure 17. The SWH scatter plots (Figure 17 and later) are plotted like those of wind speed (e.g. Figure 4) except for the size of the 2-D bin which is 0.25 m × 0.25 m in the case of SWH.

It is clear from Figure 17 that the agreement between Sentinel-3A and Sentinel-3B SWH and their model counterparts is very good except for a slight overestimation at moderate to high SWH's (above ~4 m). Sentinel-3A SRAL SAR SWH has been globally unbiased compared to the ECMWF model after the implementation of processing baseline PB 2.24. **However, the implementation of PB 2.27 caused a noticeable reduction in SWH's below ~ 2 m (seems to be related to the increased number of smaller waves noticed in the Sentinel-3 PDF's of Figure 16).** Although Sentinel-3A provides practically very good SWH product, Figure 17 suggests that there is still a need for SWH fine tuning especially for smaller values (and possibly for SWH values above ~4 m). Same remarks can be made for SWH from Sentinel-3B. The global SDD between SRAL and model SWH is about 0.26 m which corresponds to less than 10% of the mean for both satellites.

The scatter plots for Sentinel-3A SAR SWH versus the model collocations discriminated based on their geographical locations whether in the Northern hemisphere (north of latitude 20°N), the Tropics (between latitudes 20°S and 20°N) or the Southern hemisphere (south of latitude 20°S) are shown in panels (a), (b) and (c) of Figure 18, respectively, for Sentinel-3A and in panels (d), (e) and (f), respectively, for Sentinel-3B. The slight underestimation at low wave heights (after the implementation of Sentinel-3A PB 2.27) is obvious especially in the Tropics and the Southern Hemisphere. The overestimation at higher wave heights can be clearly seen at all hemispheres (although not many SWH observations exceeding 4 m in the Tropics).

The time series of the global mean and standard deviation (SD) of the SWH from Sentinel-3A and Sentinel-3B averaged over a 7-day time window moved by 1 day at a time are shown in the upper and lower panels, respectively, of Figure 19. The corresponding time series of the model as collocated with Sentinel-3A are also shown for comparison. The time series of model collocated with Sentinel-3B are similar to the shown one.

Sentinel-3A mean and standard deviation are not much different than those of the model (and the other altimeters). Sentinel-3A SWH standard deviation is slightly higher than that of the model (and the other altimeters; not shown). At the scale of the super-observations (~75 km), standard deviations of SWH are expected to almost equal as the higher resolution of SAR altimetry compared to the conventional altimetry (LRM) should not have any impact at the 75-km scale. Therefore, this higher Sentinel-3 SWH variability needs to be monitored closely to see if SWH fine tuning is needed to compensate for this enhanced variability. Figure 19 suggests that the implementation of Sentinel-3A PB 2.24 reduced the mean of the SAR SWH and made it to be in line with model mean values.

Sentinel-3B global SWH mean and standard deviation are very close to those of Sentinel-3A. However, it seems that Sentinel-3B SWH is marginally lower than that of Sentinel-3A. Although it is too small (about 1 cm), this difference is rather systematic (Figure 19).

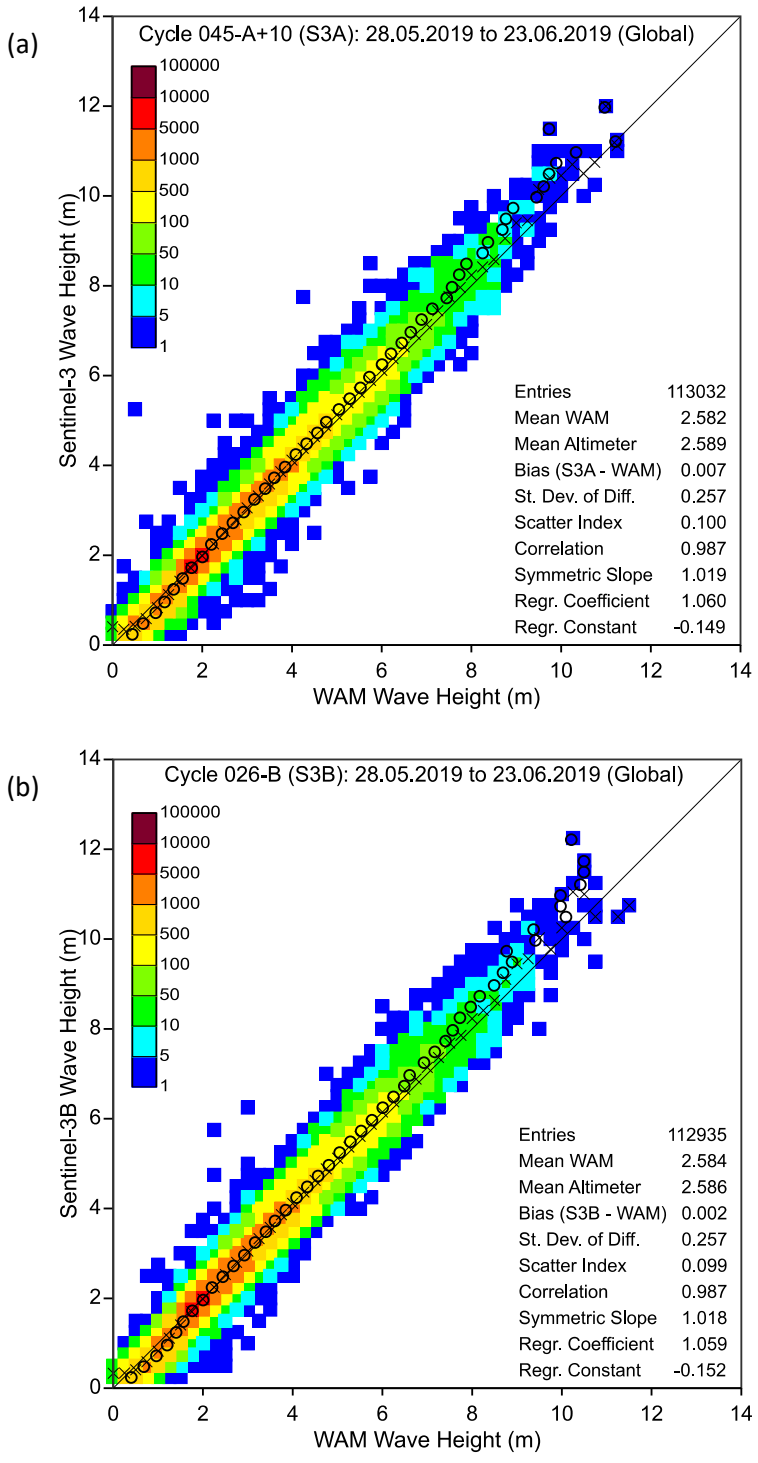

Figure 17: Global comparison between Sentinel-3 and ECMWF model first-guess significant wave height values over the period from 27/05/2019 to 23/06/2019 which corresponds to a 10-day shifted-ahead Cycle 045 (045+10) of Sentinel-3A (a) and Sentinel-3B Cycle 026 (b). The number of colocations in each 0.25 m x 0.25 m 2D bin is coded as in the legend. Refer to Figure 4 for the meaning of the crosses and the circles.

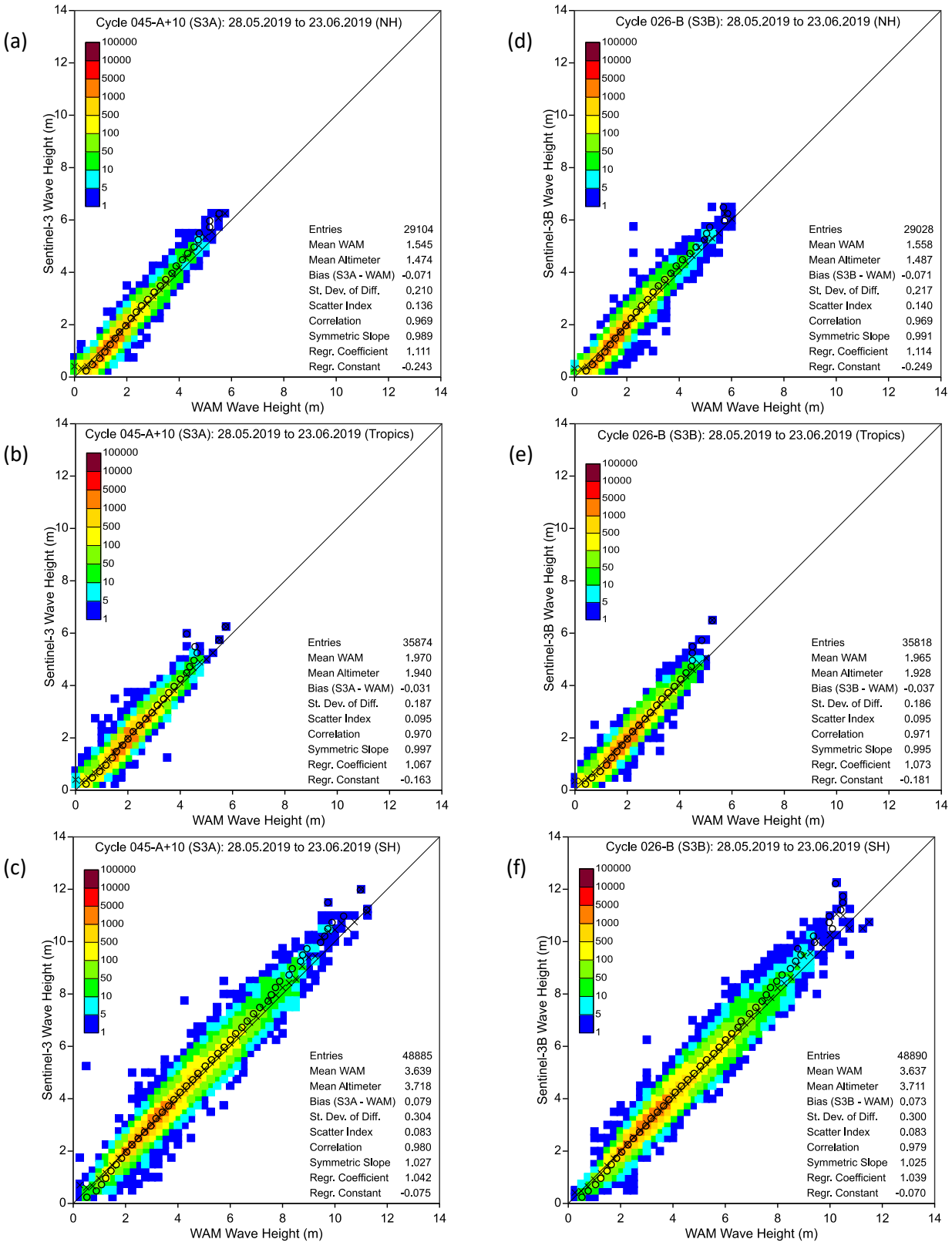

Figure 18: Same as Figure 17 but for Northern Hemisphere (latitudes to the north of 20°N), Tropics (latitudes between 20°S and 20°N) and Southern Hemisphere (latitudes to the south of 20°S), respectively.

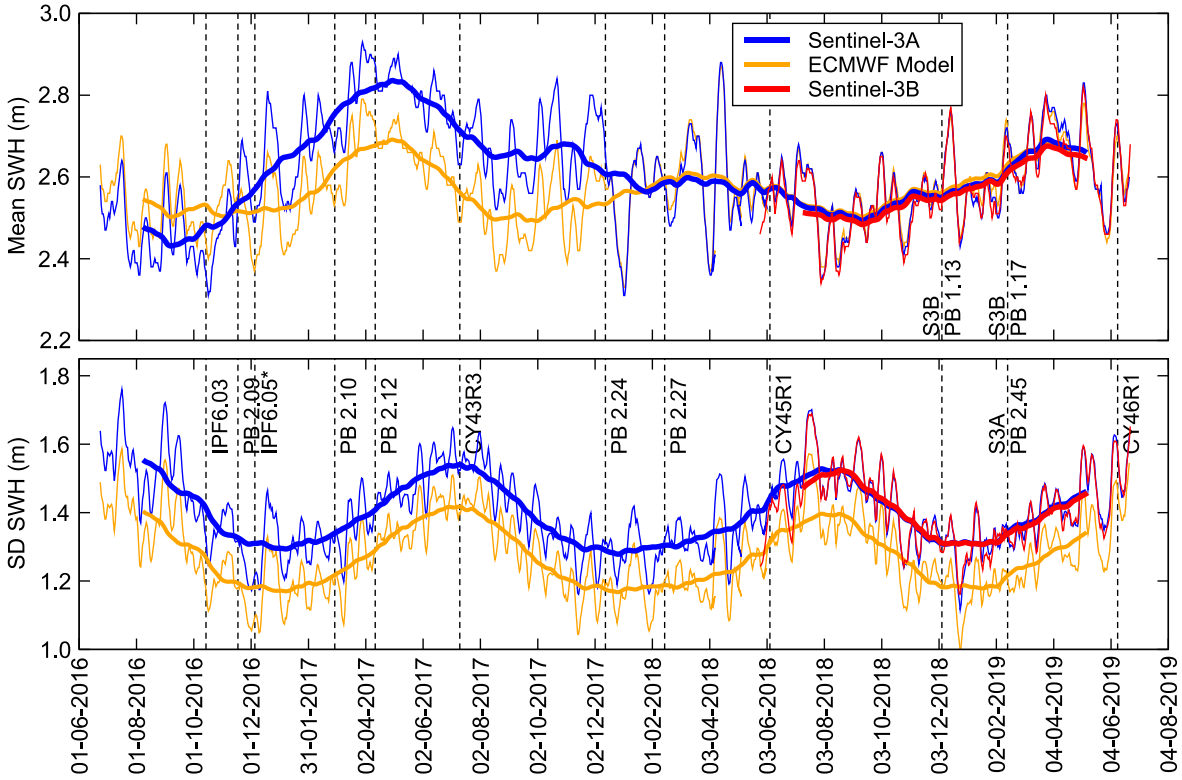

Figure 19: Time series of global mean (top) and standard deviation (bottom) of significant wave height from SRAL Ku-band after quality control. The collocated ECMWF model SWH mean and SD are also shown. The mean and SD are computed over a moving time window of 7 days and are shown as thin lines. The 92-day running means are shown as thick lines.

The time series of the SWH weekly bias (altimeter – model) and SDD of Sentinel-3A compared to the ECMWF model FG are shown in the upper and lower panels, respectively, of Figure 20. Similar timeseries plots of Sentinel-3B are shown in Figure 21

Until the first week of November 2016, Sentinel-3A used to underestimate (negative bias) SWH by about 0.05 m globally, ~0.15 m for Northern Hemisphere and the Tropics while it used to overestimate SWH in the Southern Hemisphere. A change in statistics happened in mid-November 2016 which is the time of the start of PB 2.09 implementation. This led to an increase in Sentinel-3A SWH and resulted in positive bias (SRAL higher than the model) almost everywhere. However, this change had minor impact on the SDD. Associated changes implemented late November and early December 2016, do not seem to have any impact on Sentinel-3A SWH statistics. This is the case for other changes since then until Sentinel-3A PB 2.24 which was implemented on 13 December 2017. Since then, Sentinel-3A SAR SWH has been virtually unbiased on the global scale. **However, there are very small SWH biases in the extra-tropics that follow a seasonal cycle with its maximum and minimum are occurring during the hemispheric winter and summer, respectively. The amplitude is less than 0.1 m. In the Tropics, the bias is fluctuating between -0.05 and -0.10 m. Sentinel-3A PB 2.27 seems to introduce a slight negative bias**

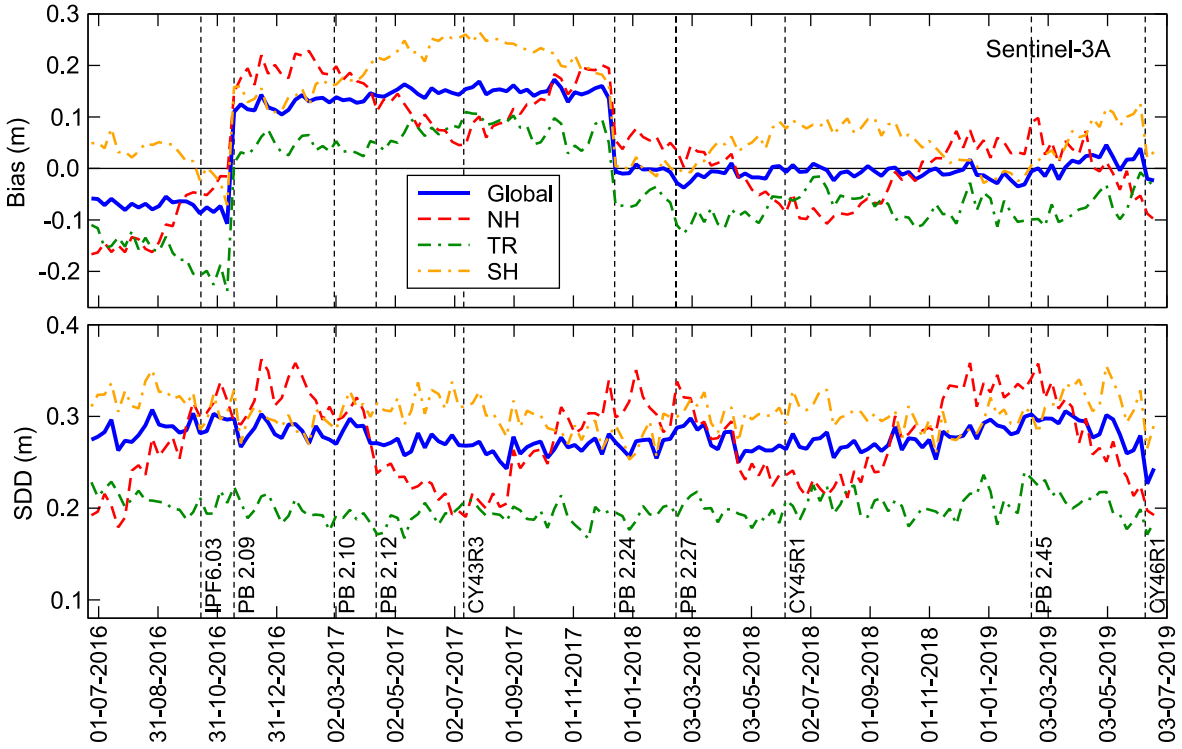

Figure 20: Time series of weekly global significant wave height bias defined as altimeter - model (top) and standard deviation of the difference (bottom) between SRAL and ECMWF model first-guess.

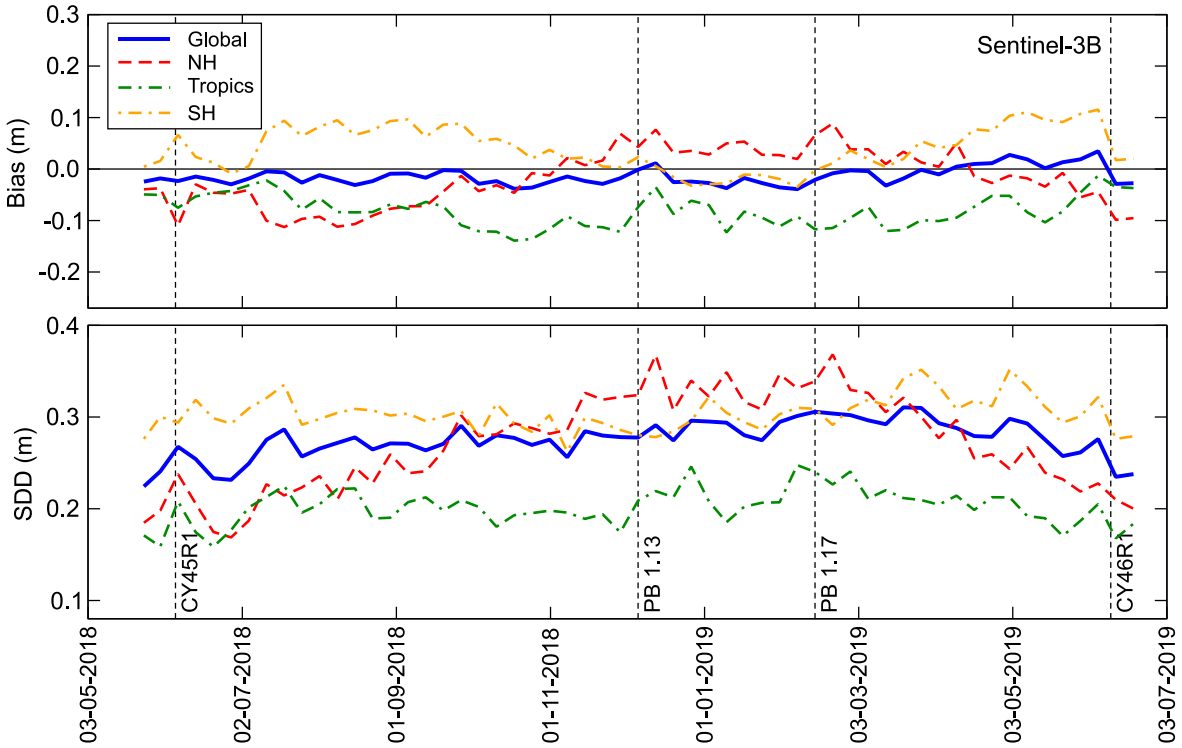

Figure 21: Same as Figure 20 but for Sentinel-3B.

especially in the NH. Both Sentinel-3A PB 2.24 and PB 2.27 do not have any impact on SDD which also follows a seasonal cycle in the extra tropics similar to that of the bias. The seasonality is stronger in the NH with an amplitude of about 0.15 m compared to about 0.05 in the SH. In the Tropics, the SDD is stable at about 0.2 m.

Sentinel-3B SWH bias is rather small since the beginning (see upper panel of Figure 21). Globally, this small bias has been consistently negative. The SWH SDD between Sentinel-3 and the model shows linear increasing trend since the beginning (see lower panel of Figure 21). **It is still too early to draw any conclusion whether this is a trend or part of a seasonal cycle.**

The implementation of the new ECMWF model (CY46R1) that involves a significant improvement in treating the swell dissipation was realised on 11 June 2019. Its impact can be clearly seen in the reduction of the SDD between Sentinel-3 data and the model. This confirms the evaluation done before the operational implementation.

The geographical distribution of the mean Sentinel-3A SWH and the SWH bias, SDD and SI with respect to the ECMWF model averaged over the period from 27/05/2019 to 23/06/2019 which corresponds to a 10-day shifted-ahead Cycle 045+10 of Sentinel-3A are shown in Figure 22. The corresponding maps from Sentinel-3B Cycle 026 are shown in Figure 23. All the four plots for both satellites look like their counterparts from other altimeters (not shown). The impact of Sentinel-3A PB 2.24 can be appreciated by comparing panel (b) of Figure 22 to the corresponding plots from the cycles before Cycle 025-A. While positive SWH bias with respect to the model was dominating the whole globe, now one can see both positive and negative (relatively small) biases.

The comparison against in-situ (mainly buoy) observations is shown in Figure 24. SRAL Ku-band SAR SWH shows **virtually no bias (bias of 0.02 and 0.04 m for Sentinel-3A and Sentinel-3B, respectively) compared to the in-situ observations for the cycles considered here. The symmetric slope for both altimeters is around 1.00.** The SDD (a proxy to the random error) values are 0.22 and 0.21 m for Sentinel-3A and Sentinel-3B, respectively. These values correspond to about 12.3% and 12.0% of the mean for Sentinele-3A and Sentinel-3B, respectively. These values are in line with the statistics usually emerge from similar comparisons. In general, SWH product from Sentinel-3A and Sentinel-3B is as good as those from other altimeters and in-situ observations (not shown). **The underestimation at low wave heights is visible in both panels of** Figure 24. It is important to state that most of in-situ observations are in the Northern Hemisphere around the American and European coasts and, therefore, the results of the in-situ comparison may not represent the global conditions very well.

The impact of the processing chains Sentinel-3A PB 2.45 and Sentinel-3B PB1.17, implemented operationally on 14 February 2019, is rather neutral.

(a)

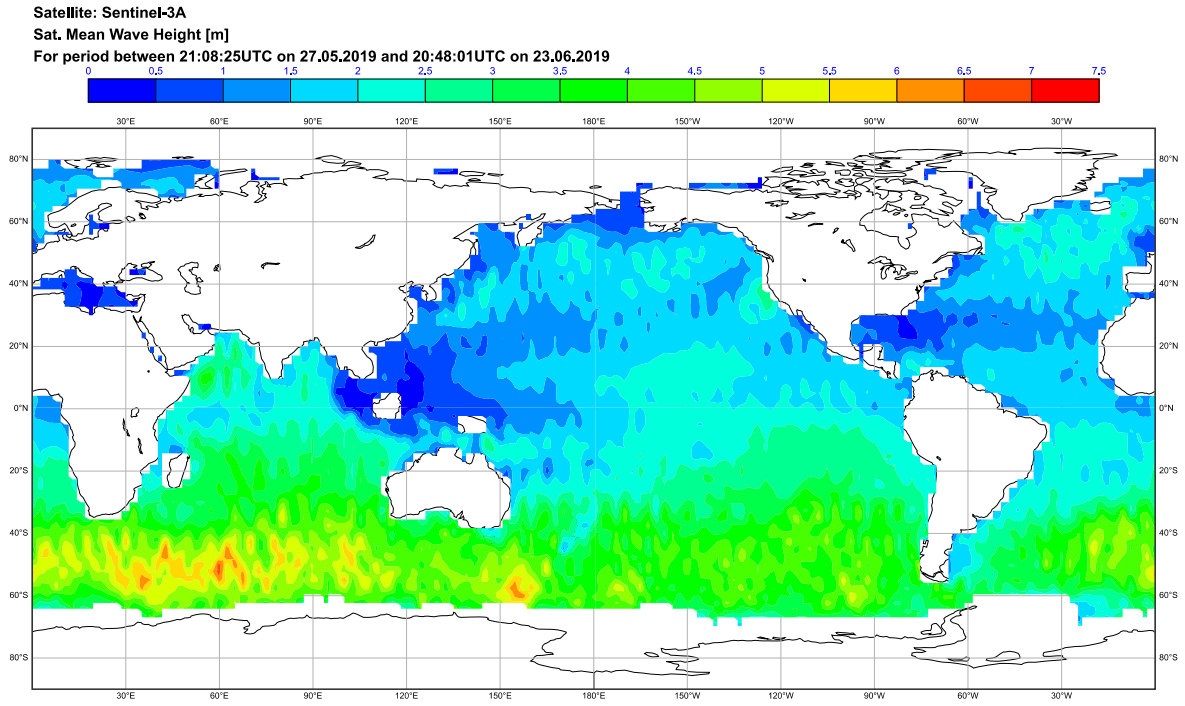

(b)

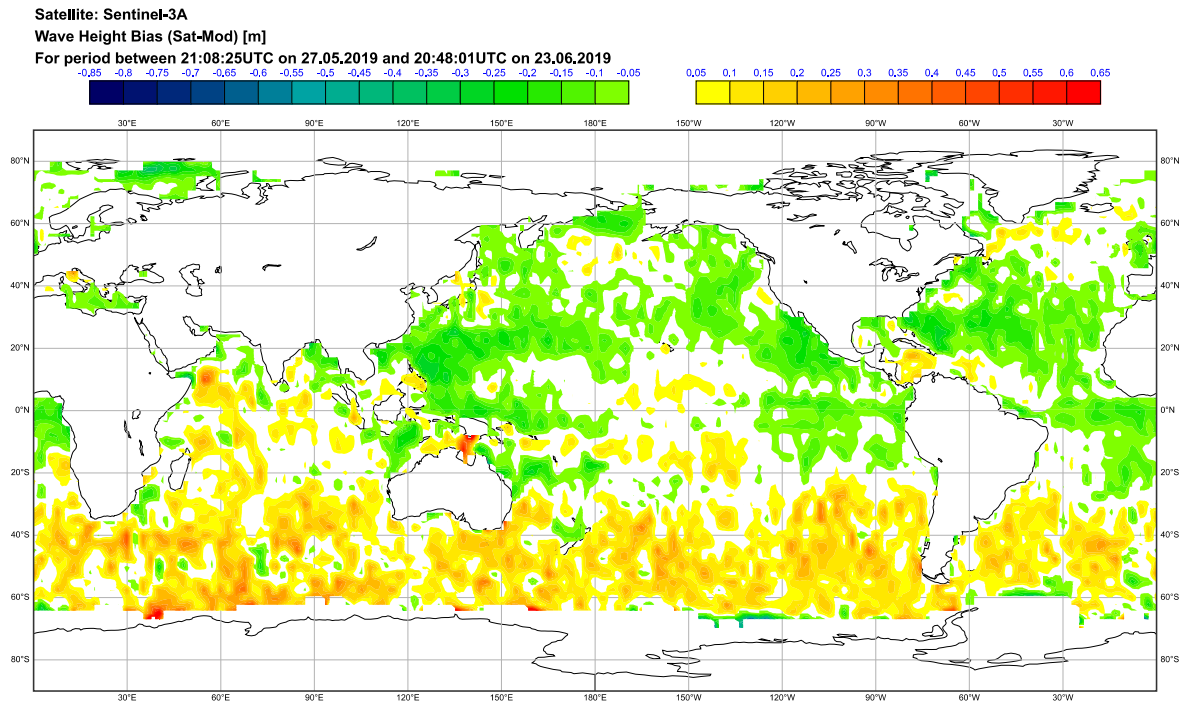

Figure 22: Geographical distribution of mean Sentinel-3A SWH (a) as well as the bias (b); the SDD (c) and the SI (d) between Sentinel-3 and ECMWF model FG during the period from 27/05/2019 to 23/06/2019 which corresponds to a 10-day shifted-ahead Cycle 045 (045+10) of Sentinel-3A. Bias is defined as altimeter – model.

(c)

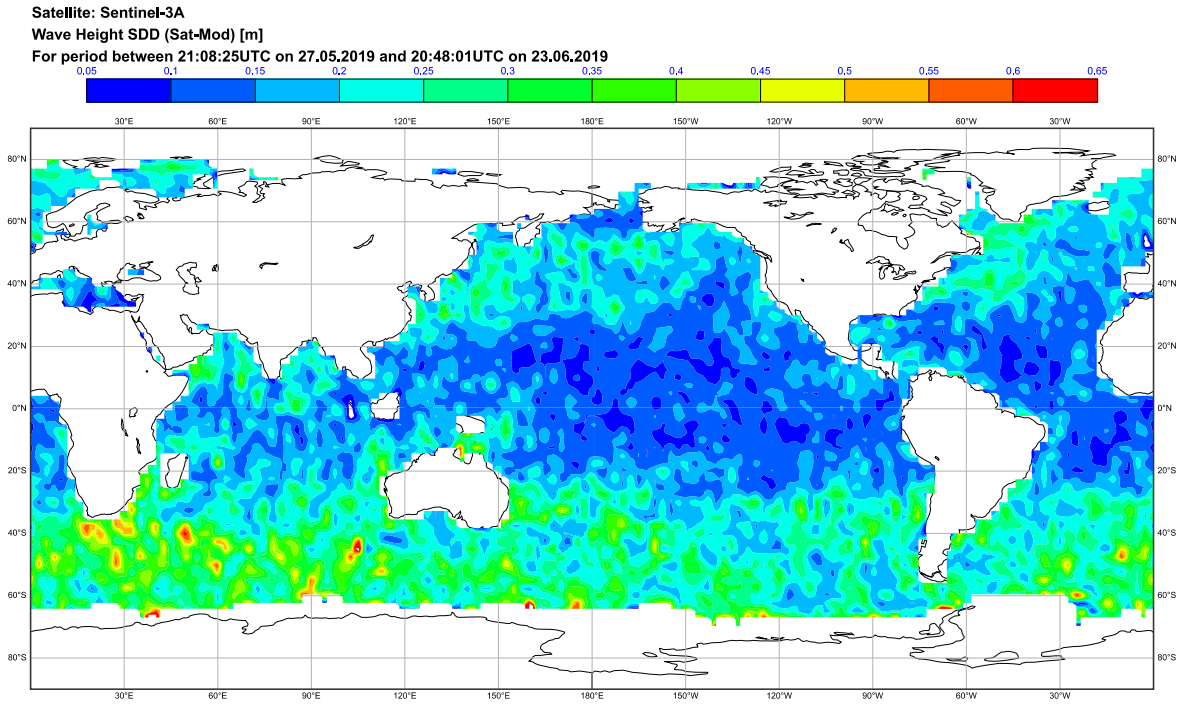

(d)

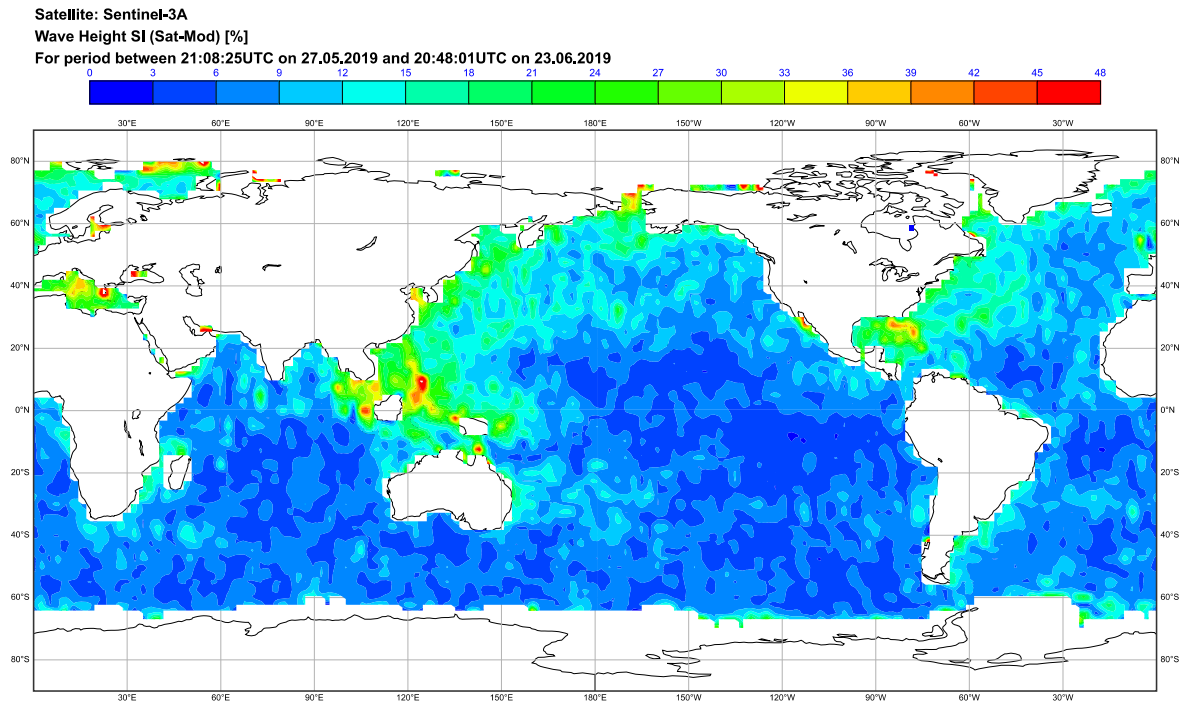

Figure 22: Continued.

(a)

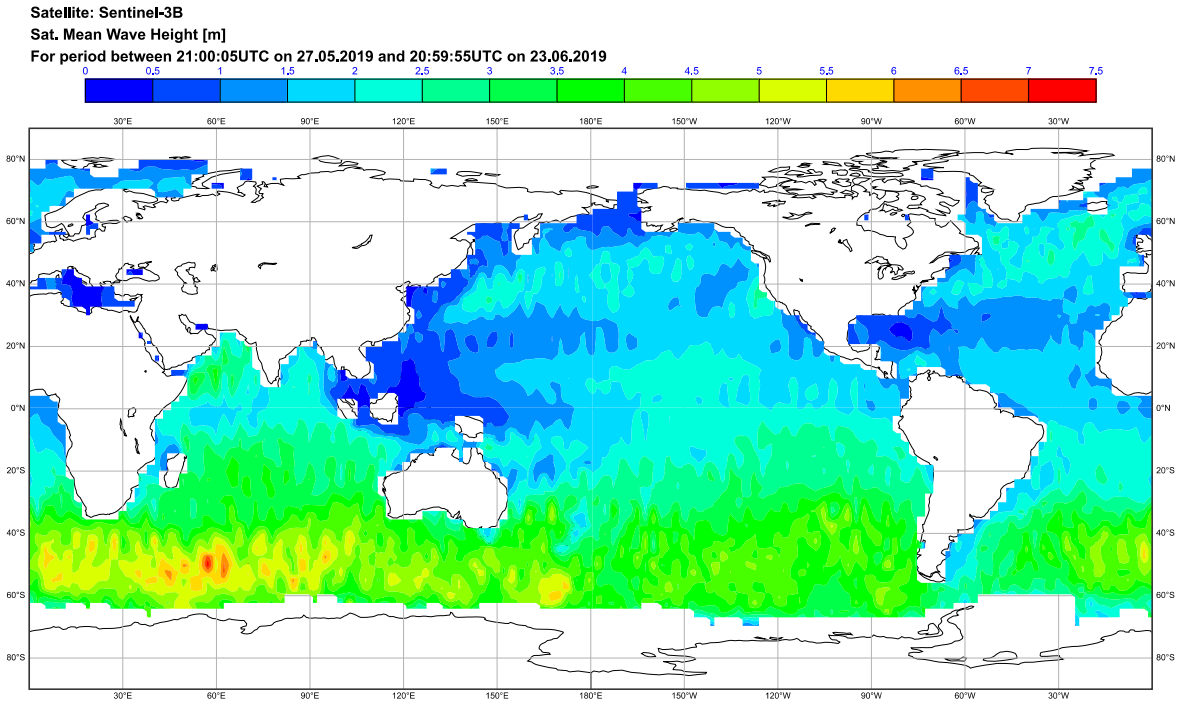

(b)

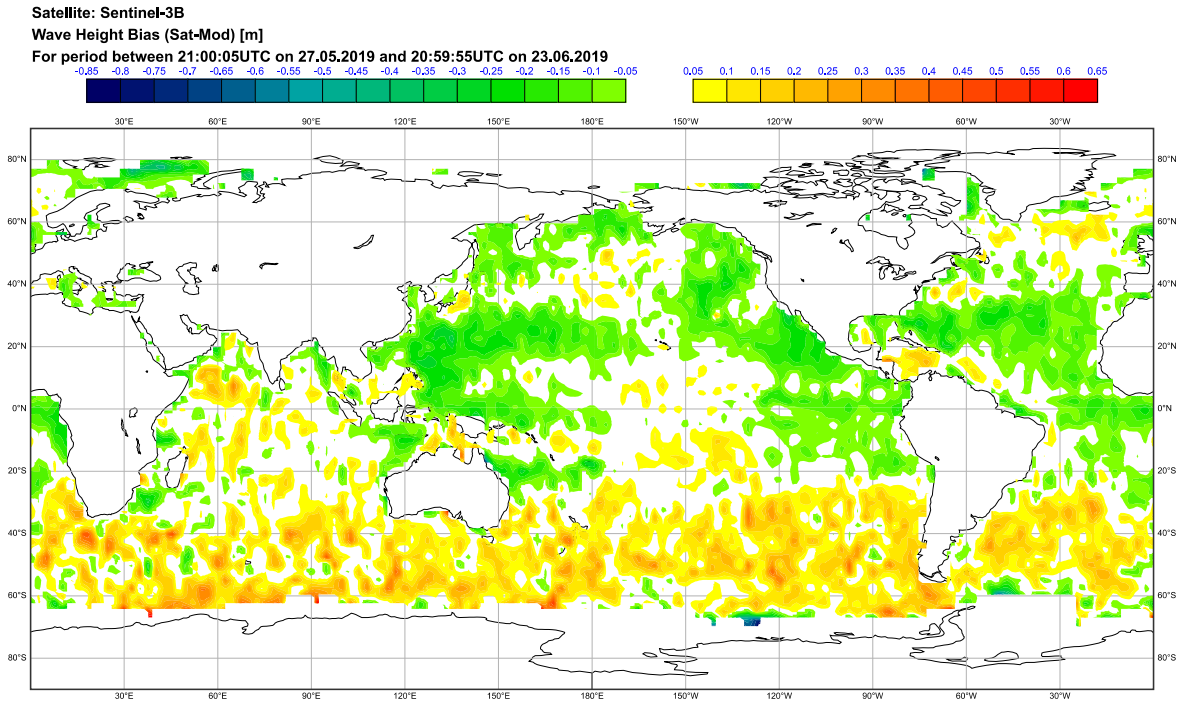

Figure 23: Same as Figure 22 but for Sentinel-3B Cycle 026 from 27/05/2019 to 23/06/2019.

(c)

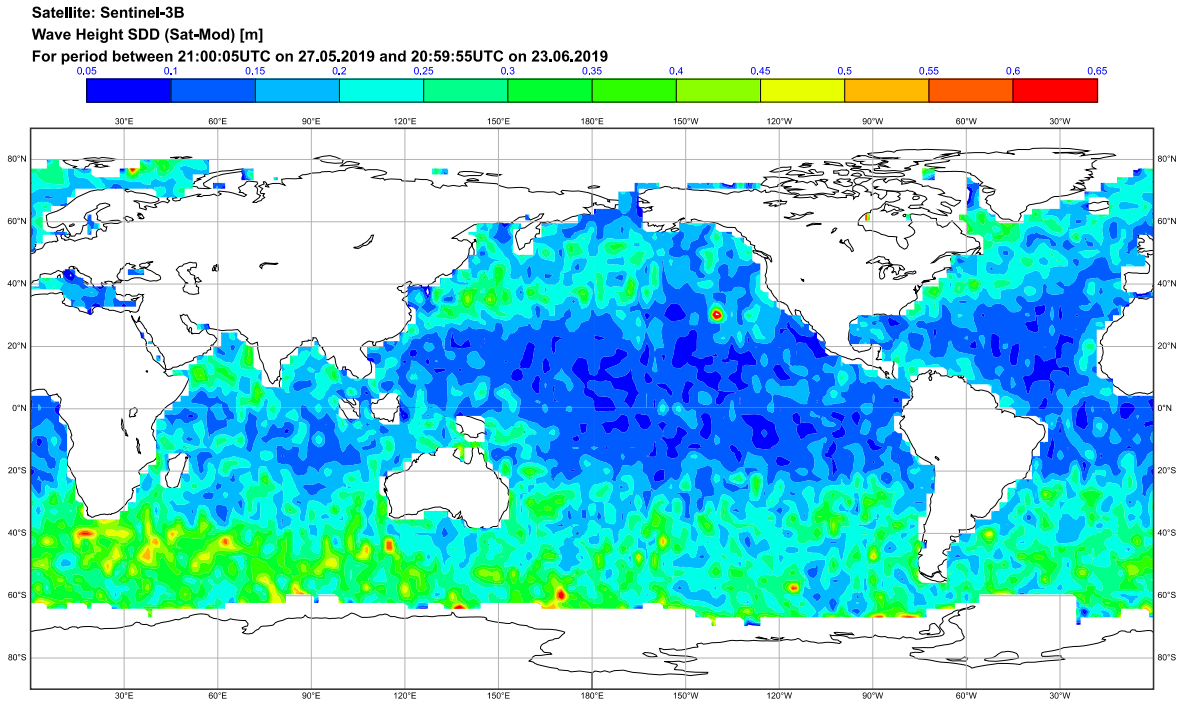

(d)

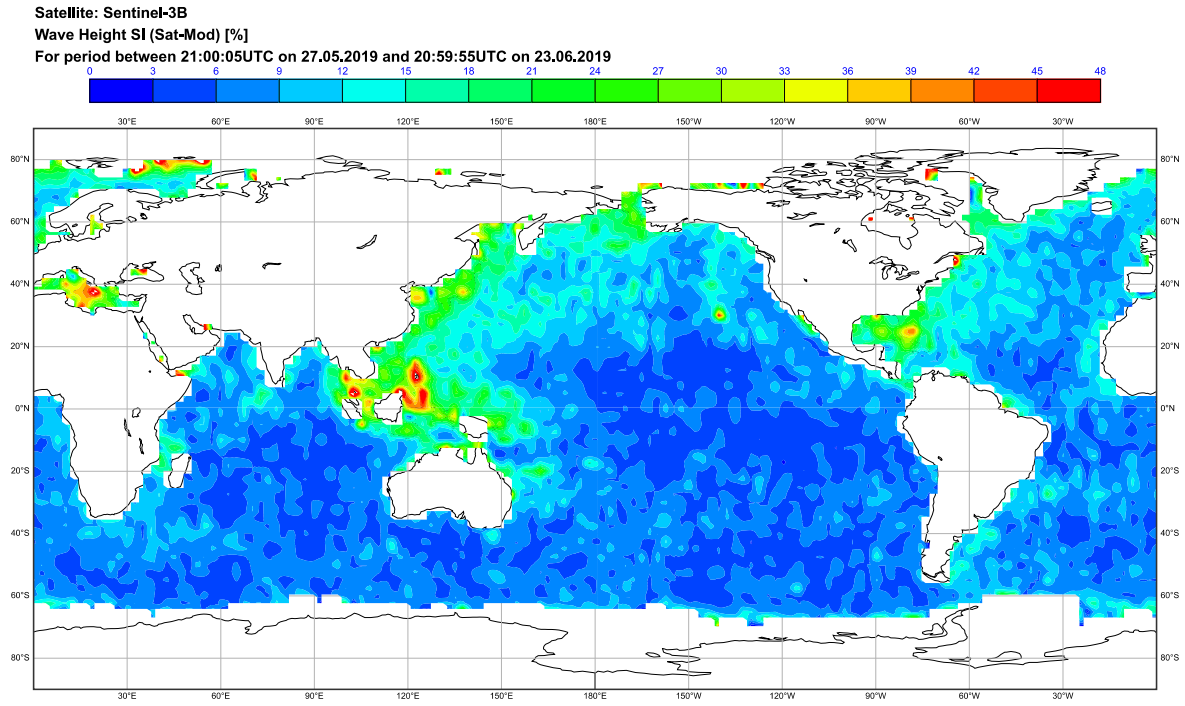

Figure 23: Continued.

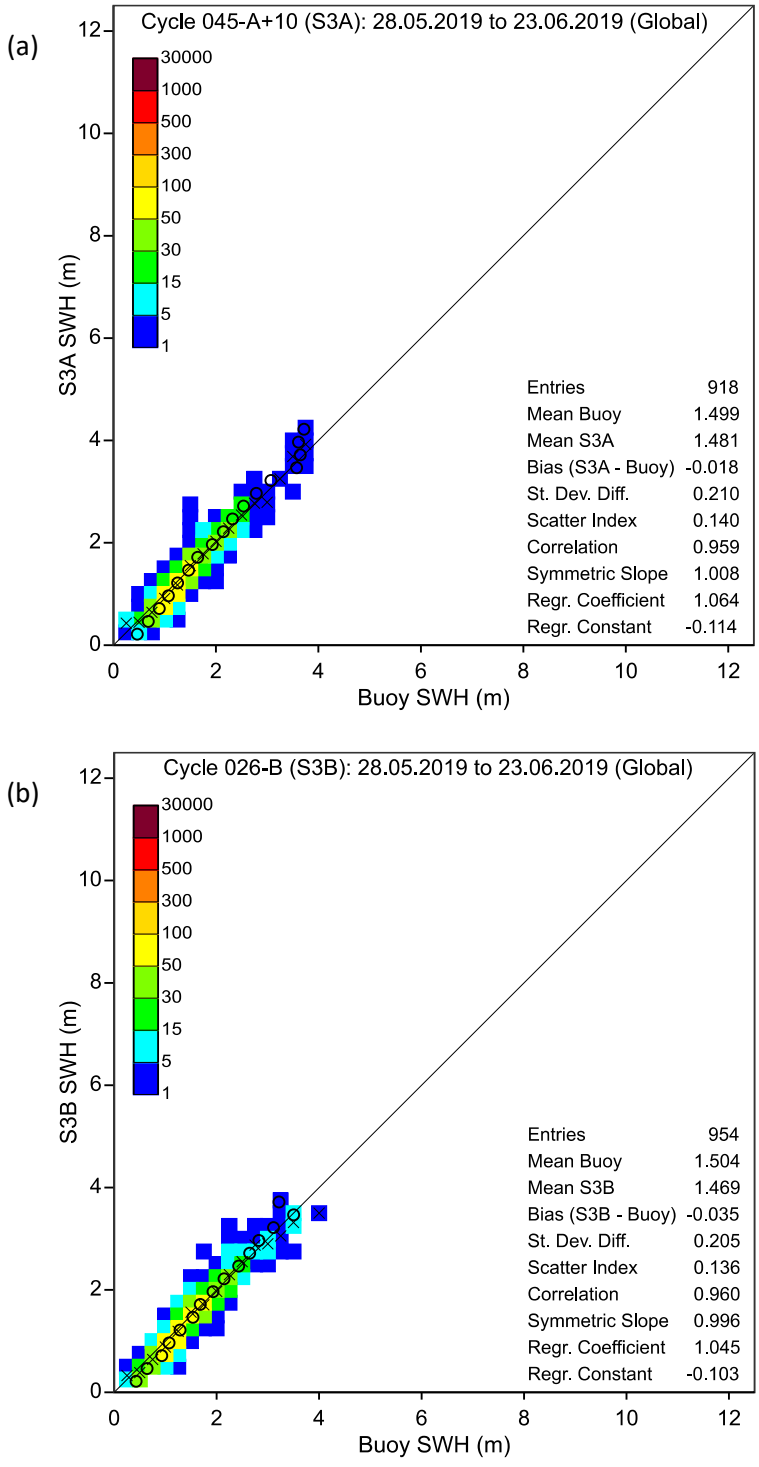

Figure 24: Same as Figure 17 but the comparison is done against in-situ observations (mainly in the NH).

6 Conclusions

Surface wind speed, PLRM wind speed and significant wave height (SWH), which are part of Level 2 Marine Ocean and Sea Ice Areas (SRAL-L2MA) also referred to as S3A_SR_2_WAT product of Sentinel-3A Radar Altimeter (SRAL) have been monitored and validated against the corresponding parameters from ECMWF Integrated Forecast System (IFS) and other altimeters. The periods considered in this report are as follows:

- Sentinel-3A for Cycle No. 045 (period from 17/05/2019 to 13/06/2019) although the period was shifted by 10 days for several plots (referred to as Cycle 045+10) to coincide with Sentinel-3B Cycle No. 026; and
- Sentinel-3B for Cycle No. 026 (period from 27/05/2019 to 23/06/2019).

The data were obtained from the Copernicus Online Data Access (ODA) service of EUMETSAT.

For Sentinel-3A, the impact of the processing chain IPF 6.03 which was implemented on October the 14th seems to be very small. However, the statistics show clearly that the IPF changes during November and December 2016 (processing baseline PB 2.09) have more impact. The first happened in middle of November, another one at the end of November and the last is at the beginning of December 2016. The processing baseline PB 2.10 has a positive impact on wind speed. Later processing change of PB 2.12 does not seem to have any significant impact. **However, the implementation of PB 2.24 (13 December 2017) caused an increase in the backscatter and a reduction in SWH. The impact on wind speed seems to be neutral (comparisons against other altimeters suggest a slight improvement). On the other hand, PB 2.27 (implemented on 14 February 2018) does not seems to have any impact except for a slight degradation of SWH for wave heights below ~ 1 m.**

The current quality of SAR wind speed, PLRM wind speed and SWH from Sentinel-3A and Sentinel-3B SRAL can be summarised as being very good and they can be used for practical applications. However, some fine tuning of these products may still be needed to alleviate some of their imperfections:

- **The new ECMWF model version (CY46R1), that was implemented on 11 June 2019, show a significant improvement in wave height comparison especially for areas dominated by swell.**
- **There is strong indication that the global mean backscatter (and wind speed) follow a seasonal cycle since mid-2018.**
- The SAR wind speed is now globally unbiased compared the wind speeds from the model and the other altimeters. The standard deviation of the difference (SDD) between SAR and model wind speeds is as good as that of other altimeters. There is a seasonal cycle in both bias and the SDD between SAR wind and ECMWF model in Northern (minimum in July and maximum in January) and Southern (vice versa) Hemispheres.
- The PLRM wind speed is now globally unbiased. The SDD with respect to the model reduced considerably recently and it is now in line with its counterpart for other altimeter winds. With the removal of the large outliers, the SDD is rather stable. A seasonal signal in the PLRM wind

bias with respect to the model like that of SAR wind can be clearly noticed. SDD of PLRM does not show a similar clear signal.

- **There has been a clear drop in the SDD between PLRM and model winds since early September 2018.**
- **After the implementation of Sentinel-3A processing baseline PB 2.24 (on 13 December 2017) Sentinel-3 SAR significant wave height became virtually unbiased compared to the model and the in-situ measurements (although the bias against in-situ measurements for this and the previous cycles was not small). However, SRAL still overestimates high wave heights slightly according to the comparison with the ECMWF model.**
- **The implementation of Sentinel-3A PB 2.27 (on 14 February 2018) caused reduction in small wave heights below ~ 1 m.**
- **The characteristics of Sentinel-3B wind and wave data are very like those of Sentinel-3A after the implementation of Sentinel-3B PB 1.13 on 6 December 2018 which eliminated the backscatter bias that degraded the wind speed products.**
- **The overall quality of the wind and wave data for Sentinel-3A Cycle No. 045 does not differ from that of the last few cycles. Similarly, the quality of wind and wave products from Sentinel-3B Cycle No. 026 is like that of the previous few cycles.**
- At this stage, it is too early to assess the impact of the processing chains, namely: Sentinel-3A PB 2.45 and Sentinel-3B PB1.17, implemented operationally on 14 February 2019.

7 References

Abdalla, S. (2005). Global Validation of ENVISAT Wind, Wave and Water Vapour Products from RA-2, MWR, ASAR and MERIS. *Final Report for ESA contract 17585*. ECMWF, Shinfield Park, Reading, RG2 9AX, UK. Available online at: http://www.ecmwf.int/en/research/publications

Abdalla, S. (2011). Global Validation of ENVISAT Wind, Wave and Water Vapour Products from RA-2, MWR, ASAR and MERIS (2008-2010). *Final Report for ESA contract 21519/08/I-OL*. ECMWF, Shinfield Park, Reading, RG2 9AX, UK. Available online at: http://www.ecmwf.int/en/research/publications

Abdalla (2015). SARAL/AltiKa Wind and Wave Products: Monitoring, Validation and Assimilation, *Mar. Geod.*, **38(sup1)**, 365-380, doi: 10.1080/01490419.2014. 1001049.

Abdalla, S. and Hersbach, H. (2004). The technical support for global validation of ERS Wind and Wave Products at ECMWF. *Final Report for ESA contract 15988/02/I-LG*. ECMWF, Shinfield Park, Reading, RG2 9AX, UK. Available online at: http://www.ecmwf.int/en/research/publications

Abdalla, S., Janssen, P. A. E. M., and Bidlot, J.-R. (2010), Jason-2 OGDR Wind and Wave Products: Monitoring, Validation and Assimilation, *Mar. Geod.*, **33(sup1)**, 239-255.

Abdalla, S., Janssen, P. A. E. M. and Bidlot, J. R. (2011). Altimeter Near Real Time Wind and Wave Products: Random Error Estimation, *Mar. Geod.*, **34(3-4)**, 393-406.

Abdalla, S., Isaksen, L., Janssen, P. A. E. M. and Wedi, N. (2013). Effective Spectral Resolution of ECMWF Atmospheric Forecast Models, *ECMWF Newsletter*, **137**, 19-22.

Bauer, E., Hasselmann, S. Hasselmann, K. and Graber, H. C. (1992). Validation and assimilation of Seasat altimeter wave heights using the WAM wave model, *J. Geophys. Res.*, **97(C8)**, 12671-12682.

Janssen, P. A. E. M. (2004). *The interaction of ocean waves and wind*. Cambridge Univ. Press, 300p.

Janssen, P. A. E. M., Lionello, L. Reistad, M. and Hollingsworth, A. (1989). Hindcasts and data assimilation studies with the WAM model during the Seasat period, *J. Geophys. Res.*, **94(C1)**, 973-993.

Janssen, P. A. E. M., Abdalla, S., Hersbach, H. and Bidlot, J.-R. (2007). Error estimation of buoy, satellite, and model wave height data, *J. Atmos. Oceanic Technol.*, **24**, 1665–1677.

8 Appendix A: Verification Approach

8.1 Introduction

The wind and wave data collected by Sentinel-3 Radar Altimeter (SRAL) are downloaded in netCDF format which is converted into ASCII format. (In the future BUFR format will be received through the Global Telecommunication System, GTS, in near real time, NRT, and will be used directly). This product is monitored daily. The product passes through the quality control procedure described below. The data then are collocated with and verified against the model fields produced by the ECMWF integrated forecasting system (IFS) which includes an atmospheric model and a wave model (WAM) and runs operationally twice a day.

In general, the altimeter significant wave height values that pass the quality control (QC) are assimilated into the operational ECMWF wave model. This assimilation is important to improve the "nowcast" of the model and to provide more accurate initial condition for the medium-range wave forecast (up to 15 days). The altimeter wind speed data are not assimilated into the ECMWF atmospheric model. Therefore, the wind speed information is used as a diagnostic tool for the model output and the model wind speed can be used as an independent verification for the altimeter data.

The best estimate of the weather conditions (which is the model analysis) is used to verify the altimeter wind speed as it is not assimilated in the model. On the other hand, SWH which is usually assimilated in the model are verified against the model first guess (the model state just before the assimilation process). Even if the altimeter SWH product to be verified is not assimilated, the assimilation of SWH from other altimeters still cause error correlation as all altimeter products share the same principle of measurement (Janssen et al., 2007).

Furthermore, the altimeter data are collocated with and verified against available in-situ wave buoys and platform wind and wave measurements which are received at ECMWF through the GTS on weekly and monthly bases. The results of this performance monitoring and geophysical validation are summarised in this monthly report series.

Table A.1: QC Parameters for Altimeter Data from Various Satellites

Satellite	RAW	FLG	1-Hz Δ	N_{max}	N_{min}
ERS-1/2	URA	RFL	7 km	30 (=210 km)	20
ENVISAT	WWV	RF2	7 km	11 (= 77 km)	7
Jason-1	JAS	RFJ	6 km	13 (= 78 km)	8
Jason-2	JA2	RJ2	6 km	13 (= 78 km)	8
Jason-3	JA3	RJ3	6 km	13 (= 78 km)	8
Cryosat-2	CSE	RFC	7 km	11 (= 77 km)	7
SRAL/AltiKa	KAB	RFS	7 km	11 (= 77 km)	7
Sentinel-3A	S3A	RFA	7 km	11 (= 77 km)	7

8.2 Quality Control Procedure

The altimeter wave height and wind speed data are subject to a quality control (QC) procedure to eliminate all suspicious measurements. The procedure was first suggested by Janssen et al. (1989) and Bauer et al. (1992) for the SeaSat altimeter data. The procedure was enhanced later and used for ERS-1, ERS-2 (see Abdalla and Hersbach, 2004), ENVISAT (Abdalla, 2005 and 2011), Jason-1, Jason-2 (Abdalla et al., 2010 and 2011), Cryosat-2 and SARAL/AltiKa (Abdalla, 2015) altimeter data.

The daily altimeter data stream is collected for time windows of 6 hours centred at the 4 major synoptic times. Currently monitoring suites are run after the end of day "yyyymmdd", where yyyy is the year, mm is the month, dd is the day, considering time windows centred at 18:00 UTC of previous day and 00:00, 06:00 and 12:00 UTC on that specific day. This configuration is implemented to go in parallel with the ECMWF operational system. The raw data are stored in a file with the internal naming convention of "RAWyyyymmddhhnn", where RAW is a 3-letter prefix identifying the satellite or product (see Table A.1) while hh and nn are the hour and the minute, respectively, of the centre of the time window. This file is nothing but the original product (usually in in BUFR format) for the whole time window starting 3 hours before the time of the centre of the window (i.e. time "yyyymmddhhnn") and ending 3 hours afterwards.

The quality control (QC) procedure is divided into two processes:

1. A basic process: to ensure that each individual observation is within the logical range and is collected over water, during the correct time window.

2. A secondary process: to ensure that observations within any given sequence are consistent with each other. This process is only applied on observations passing the first process.

It is important to mention that this classification is just for clarification purposes and has no consequence on the quality control procedure itself.

8.3 Basic Quality Control

The RAW product is first decoded. Any record with missing value of any key parameter (i.e. time, location, backscatter, significant wave height, ... etc.) is considered as a corrupt record and is discarded (as if it does not exist). The records belong to the current time window but found in the files of the previous windows (see below), are read in (if any). All the observation records are then sorted according to the acquisition time. The records are checked to detect any duplicated observation. One of those duplicates is retained while the other(s) is/are rejected by setting the "*double-observation flag*" which is the general quality flag number 4 (Table A.2).

If the peakiness factor, which is a measure of the degree of peakiness in the return echo and is supplied as part of the RAW product, is very high, the record should be rejected as this is an indication of the existence of sea ice contaminating the observation. The threshold value for the peakiness factor is selected as 200 based on some empirical numerical tests for ERS-2. The peakiness factor in this context is defined as:

Table A.2: The Standard Quality Flags used in the Quality Control Procedure. A flags is raised (i.e. set to 1) to indicate an issue. An observation record passes QC if all general flags except flag 6 are not raised (i.e. set to zero). SWH and wind speed have their own specific flags.

General Flags

Flag #	Quality Flag Name	Meaning
1	Time window	Record belongs to another time window
2	Land point	Record over land (model land-sea mask)
3	Grid area	Record outside the WAM model grid
4	Double observation	Duplicate observation
5	Peakiness/ Range SD	Std. dev. of main band range > threshold or peakiness* > threshold or ice flagged
6	As above for band2*	Std. dev. of 2nd band range* > threshold
7	Rain flag*	Rain contamination* (if applicable)
8	Data gap	Jump before or after a gap (e.g. island)
9	Short sequence	Too few of accepted records in a sequence

Wave & Wind Flags

Flag #	Quality Flag Name	Meaning
1	SWH range	SWH out of range (< 0.1 m or > 20 m)
2	Noisy SWH	SWH variance too large in the sequence.
3	SWH confidence	SWH outside the 95% confidence interval.
4	Wind speed range	Wind speed out of range (< 0.1 m/s or > 30 m/s)
5	Noisy wind speed	Wind speed variance too large in the sequence.
6	w. speed confid.	Wind speed outside the 95% confidence interval.
7	Band2* SWH range	2nd band* SWH out of range (< 0.1 m or > 20 m)
8	Noisy band2* SWH	2nd band* SWH variance too large in sequence.
9	Band2* SWH confid.	2nd band* SWH outside 95% confidence interval.
10	Band2* short seq.	Short sequence of the 2nd band* SWH.

* *if applicable*

$$\text{Peakiness Factor} = 100\, P(t)_{max} / [2 \langle P(t) \rangle] \qquad \text{(A.1)}$$

where $P(t)$ is the echo power as a function of time t, $P(t)_{max}$ and $<P(t)>$ denote the maximum and mean values of the echo power. Therefore, if the peakiness factor exceeds the threshold value (=200), the record is rejected by setting the "*peakiness/range SD flag*" which is the general quality flag number 5 (Table A.2).

The "*peakiness/range SD flag*" which is the general quality flag number 5 (Table A.2) is also raised (set to 1) if the 1-Hz range standard deviation (from the main band which is usually the Ku-band if the altimeter has more than one band) exceeds a given threshold. The threshold was set originally as 0.2 m. This caused high rejection rates at extreme sea states and therefore was adjusted later based on careful comparison with the model and buoys to be 0.20 m + 0.015 * SWH. The same flag is also raised if an ice flag is present and raised in the RAW product.

In the case that the altimeter has a secondary channel (e.g. S-band for ENVISAT and C-band for Jason-1/2/3 and Sentinel-3), if the 1-Hz range standard deviation from the secondary channel exceeds the same threshold above, the "*band-2 peakiness/range SD flag*" which is the general quality flag number 6 (Table A.2) is raised.

If the observation is found to belong to any of the previous time windows, it is assumed that it is too late to process this observation and the record is rejected by setting the "*time window flag*" (flag number 1 in Table A.2). If the observation belongs to a later time window, the record is removed from the observation stream and written into a file that will be read while processing observations of that time window.

The observation is then mapped on the land-sea mask of the wave model (WAM) model. The used land-sea mask is an irregular (reduced) latitude-longitude grid with resolution of 0.25°(around 28 km in both directions). If the observation is mapped on a land point, the record is rejected by raising the general quality flag number 2; namely "*land point flag*" (Table A.2).

If the observation is mapped on a grid point outside the grid area (e.g. over permanent sea ice which used to be north of 81°N but not the case anymore), the record is rejected by raising the "*grid area*" flag (general flag number 3 in Table A.2).

If a "*rain contamination flag*" is available in the RAW product, this information is used to set the general quality flag number 7 which is "*rain flag* (Table A.2).

The value of the altimeter significant wave height (SWH) is checked to make sure it is within the accepted logical range. If the SWH value is found to be below the accepted minimum (a value of 0.10 m is used) or above the accepted maximum (a value of 20.0 m is used), then the record is rejected by raising the "*SWH range flag*" which is flag number 1 of the group "wave and wind flags" (Table A.2).

Similar checks are done for the wind speed and the SWH of the secondary band (if available). The corresponding flags are the "*wind speed range*" (wave and wind flag number 4) and "*band2 SWH range*" (wave and wind flag number 7) of Table (A.2). Note that both flags are raised if the SWH is rejected (e.g. "*SWH range flag*" is raised).

8.4 Consistency Quality Control

The observations that pass the basic quality control go through the second stage of quality control, which includes several consistency tests. The altimeter observations are grouped as sequences of neighbouring observations. The maximum number of individual observations within each sequence, N_{max}, is selected to form altimeter "super-observations" of the same scale as that of the model. Table (A.1) lists the values on N_{max} for various satellites. Note that N_{max} value for ERS-1 and ERS-2 is 30. This selection was made in the early days of the ERS missions when the grid resolution of the ECMWF WAM model was 3 degrees (about 330 km) and later reduced to 1.5 degrees (more than 150 km). The value of 30 was never changed to maintain comparability. For reprocessing, it is suggested to change that value to 11.

The sequence construction starts by selecting the first record that passes the basic quality control in the time window under consideration as a possible candidate to be the first member in the new sequence. The time and the SWH observation of the next record is compared with that of the last selected record in the sequence. If the time difference between both records is more than an allowed maximum duration (3 s is used) or if the absolute difference between both SWH values exceeds an allowed maximum value (2.0 m is used), then it is assumed that there is a jump over a gap (e.g. land or sea ice). The previous record is removed from the sequence and is rejected by setting the "*data gap flag*" (the general quality flag number 8) to 1. The current record then becomes the first record in the sequence. The same procedure is repeated until there are two records accumulated in the sequence.

More records are recruited to the sequence in the same manner until either a gap is detected (exceeding either the maximum allowed time difference or the maximum allowed SWH difference) or until the maximum number of observations N_{max} in the sequence is reached. If a gap is detected and the number of the records accumulated in the sequence is less than a predefined minimum, N_{min}, (see Table A.1), all of the already selected records are rejected by raising the general "*short sequence flag*" (general flag 9 in Table A.2) to indicate a "*short sequence*" condition. If the number of observations in the sequence exceeds the predefined minimum (including the case that the maximum number has been reached), then the sequence goes through further quality control checks. The mean and the standard deviation of the observations accumulated in the sequence are computed.

The next step is to eliminate spikes by rejecting observations with SWH outside the 95% confidence interval. To accomplish this, we compute the SWH confidence limits of the sequence as:

$$\text{Confidence Interval} = \min \{ \alpha, \zeta \cdot \sigma \} \qquad \text{(A.2)}$$

where α is a maximum value of the confidence interval (used as 2.0 m in the first iteration and as 1.0 m in the second iteration), ζ is a factor for the spike test (a value of 3 is used), and σ is the standard deviation of SWH. If the absolute value of the difference between the SWH of the individual record and the mean SWH of the sequence exceeds the confidence interval computed by Eq. (A.2), then that individual record is rejected by raising the "*SWH range flag* (Wave & Wind flag number 3 in Table A.2). The flagged records are removed from the sequence and another spikes-removal iteration is carried out using the modified sequence and a rather stricter confidence interval condition (in Eq. (A.2), the value of 1.0 m for α is used in the second iteration).

If the number of individual records passed the spikes test in the sequence is less than the minimum allowed (N_{min} records), all the records in the sequence are rejected by raising the "*short sequence flag* (general flag number 9 in Table A.2) to indicate a "*short sequence*" condition. If there are enough records, the mean and the standard deviation of SWH, backscatter, wind speed, ... etc. are computed. Also, the mean geographical coordinates and the mean time of the sequence with the records passed the spikes test are also computed. The average value of the sequence is called "super-observation".

After that, the variance of the SWH values in the sequence is tested. The maximum allowed SWH variability within the sequence is given by:

$$\text{Maximum SD} = \max \{ \beta, \gamma \cdot \mu \} \qquad \text{(A.3)}$$

where β is the minimum allowed standard deviation (0.5 m is used), γ is a factor for the variance test (0.5 is used) and μ is mean value of SWH in the sequence. If the standard deviation of the SWH exceeds the maximum value computed by (A.3), all records in the sequence are rejected by raising "*Noisy SWH flag*" which is Wave & Wind Flag number 2 in Table A.2) to indicate a "*noisy observation-sequence*" condition.

The same last action is repeated on the surface wind speed (instead of SWH) and the corresponding flags (Wave & Wind flags 4 to 6 in Table A.2) are raised if needed. Similar action is done on the SWH (or wind speed) from the secondary band if one is available. The corresponding Wave & Wind flags 7 to 10 in Table A.2) are raised if needed.

The same whole procedure is repeated by selecting a new sequence until all the observations within the current time window are processed.

8.5 Output Files

The quality control procedure described above generates two types of files: "Radar flagged" (RFL) file, and "Radar averaged" (RAV) file. Furthermore, it appends a record in an "extended statistics file" (ESF) for each time window representing the statistics of quality control procedure for that specific window. The ESF file is used to plot the time series of data received, data rejections and data acceptance.

All records processed are written together with their corresponding flags in the "Radar flagged" file with the following naming convention: "FLGyyyymmddhhnn", where FLG is replaced by the 3-letter prefix corresponding to the altimeter under consideration as given in Table (A.1). This file contains the complete information included in the RAW product with the values of the quality flags listed in Table (A.2) and described above. This file covers the 6-hour time period centred at time yyyymmddhhnn. This file is an important product that can be used instead of the original RAW product. For example, this file is used as the input to the data assimilation procedure where only observations passed the quality control are used in assimilation.

The super-observations (i.e. the means and standard deviations of the sequences with records passed the quality control) are written to the "Radar averaged" file with the following naming convention: "RAVyyyymmddhhnn". This file contains the sequence means and standard deviations for the whole

time window extending from time yyyymmddhhnn-3 hours to yyyymmddhhnn+3. This file is not of much practical interest as it is considered as an intermediate medium to pass the averages needed in the next step which is the altimeter-model collocation.

8.6 Altimeter Model Collocation

After the quality control and averaging process, the individual altimeter SWH observations that pass the quality control are prepared for the data assimilation. To be specific, the FLG file is used for this procedure. The individual observations within the catchment area of a grid point (i.e. within a box with dimensions of grid increment and centred on the grid point) are averaged and assigned as the SWH observation corresponding to that grid point. The model is run to produce the first-guess fields. The data assimilation procedure is then used to blend the first guess fields with the RA observations to produce the analysed fields.

The ECMWF analysis wind velocity fields and the various WAM first-guess wave (SWH, mean wave direction, mean wave period, peak wave period, ... etc.) fields are interpolated over a regular grid (e.g. 0.5° by 0.5°) at all analysis times (00:00, 06:00, 12:00, and 18:00 UTC). Each RA super-observation represented by the mean time and position of the corresponding sequence in the RAV file is collocated with the nearest model grid point. The values of the model parameters at the corresponding grid point and at the previous and next analysis times are interpolated at the mean time of the super-observation. The super-observation record and the time-interpolated model parameters are all written in the altimeter-model collocation (RAC) file. The name convention of this file is: "RACyyyymmddhhnn" covering the 6-hour time period centred at time yyyymmddhhnn.

8.7 Altimeter Buoy Collocation

In-situ wind and wave observations, which are collected by ships, buoys and platforms (for simplicity, all will be called hereafter: “buoy data”), are routinely received at ECMWF through the GTS and archived. Significant portion of the buoy data arrives with some delay. In general, most of the buoy data arrives within 48 hours of the acquisition time.

Most of the buoy observations are collected on hourly basis. The remaining part may be collected at lower frequencies (e.g. 3 hours). The buoy observations collected 2 hours earlier and later than an analysis time (5 observations) are averaged and assigned to be the buoy observation at that analysis time. This buoy observation is collocated with the nearest model grid. The averaged buoy observations and the model analysis parameters (namely: SWH, mean wave direction, peak wave period, wind speed and direction, MSL pressure, air and seawater temperatures) are written to a collocation buoy-model (CBM) file. This task is run operationally every day with a lag of two days to ensure the arrival of most of the buoy data.

The triple-collocation (RA-model-buoy collocation) exercise is done at the beginning of each month (on the 4th of the month) for the whole of the previous month. The contents of the RAC (described above) and the CBM files are used. A RAC record is collocated with a CBM record if the following two conditions are satisfied:

1. both the RA super-observation and the buoy observation are assigned to the same analysis cycle; and

2. the distance between the RA super-observation and the buoy is within a given distance (200 km is used).

Each collocated pair of records are merged as one record and written to a collocation altimeter-buoy (CAB) file. The name convention of this file is: "CAByyyymm010000" covering the whole month mm of year yyyy.

The maximum acceptable collocation distance and time interval between the collocated altimeter and buoy observation pair are rather relaxed (200 km and 2 hours; respectively). This criteria is selected to gather enough number of collocations for meaningful statistics. To reduce the risk that the collocated altimeter and buoy SWH observation pair do not represent the same ground truth, their model counterparts are required not to be different by more than 5%. Furthermore, the mean direction of wave propagation in the model at the two locations should not differ by more than 45°. This ensures the homogeneity of the sea-state conditions at least from the model point of view. The same criteria cannot be used for wind speed. For the results presented here, wind speed collocations are accepted whenever the SWH collocation is accepted. For more detailed analyses (e.g. triple collocation error estimates of wind speed), a relaxed SWH (not wind speed) maximum difference of 50% is used. The maximum allowed difference in model wind direction at the altimeter and buoy locations is set as 20°. The background of this selection for both SWH and wind speed is based on the physics of wind and wave generation and propagation. However, the specific values used here are based on experience (see, for example, Abdalla et al., 2011).

9 Appendix B: Related Reports

Other reports related to the Optical mission are:

- S3 SRAL Cyclic Performance Report, S3A Cycle No. 045, S3B Cycle No. 026 (ref. S3MPC.ISD.PR.04-045-026)
- S3 MWR Cyclic Performance Report, S3A Cycle No. 045, S3B Cycle No. 026 (ref. S3MPC.CLS.PR.05-045-026)
- S3 Ocean Validation Cyclic Performance Report, S3A Cycle No. 045, S3B Cycle No. 026 (ref. S3MPC.CLS.PR.06-045-026)
- S3 Land and Sea Ice Cyclic Performance Report, S3A Cycle No. 045, S3B Cycle No. 026 (ref. S3MPC.UCL.PR.08-045-026)

All Cyclic Performance Reports are available on MPC pages in Sentinel Online website, at: https://sentinel.esa.int

End of document